Mathematics

https://www.aimspress.com/journal/Math

AIMS Mathematics, 11(7): 22456–22494.
DOI: 10.3934/math.2026909
Received: 07 May 2026
Revised: 11 July 2026
Accepted: 14 July 2026
Published: 27 July 2026

Research article

Bilinear optimal control of a second-order-in-time fourth-order dynamical system with advection effects

Nouf A. Alrubea and Maawiya Ould Sidi

Department of Mathematics, College of Science, Jouf University, Sakaka 72441, Saudi Arabia

* **Correspondence:** Email: naalswilem@ju.edu.sa.

Abstract: This paper addresses a bilinear optimal control problem for a second-order-in-time fourth-order dynamical system with advection effects. Although bilinear control problems for parabolic and wave-type equations have been widely studied, the optimal control analysis of second-order-in-time systems involving fourth-order diffusion and drift-type bilinear controls remains less developed. This motivates the present work. The main contribution is the development of a complete optimal control framework for this class of systems. We first prove the well-posedness of the controlled state equation and establish the existence of an optimal control by using the direct method of calculus of variations. Then, we derive the first-order derivative of the reduced cost functional through a perturbation argument and characterize the optimal control by means of the associated adjoint system. We also discuss second-order necessary and sufficient optimality conditions, which provide a refined characterization of local optimality. For the numerical approximation, we construct a finite difference scheme for the state and adjoint equations and combine it with a gradient-based iterative algorithm to approximate the optimal control. The numerical experiments illustrate the decrease of the distributed and terminal tracking errors, as well as the boundedness of the control energy. These results confirm the effectiveness of the proposed approach and show its ability to steer the system toward prescribed targets with moderate control effort.

Keywords: bilinear optimal control; fourth-order dynamical system; advection control; optimality conditions; gradient descent algorithm; simulations
Mathematics Subject Classification: 49J20, 49K20, 35G35, 35Q93, 65M06

1. Introduction

The analysis and control of distributed parameter systems governed by partial differential equations constitute an important topic in dynamical systems and mathematical control theory. Such systems arise in many natural and engineering applications, including vibration control, wave propagation, heat transfer, and the dynamics of flexible structures. In these problems, the state evolves in both time and space, and finite-dimensional models are often not sufficient to capture the full behavior of the system. This motivates the use of infinite-dimensional dynamical models and PDE-constrained optimal control methods [1].

Fourth-order evolution equations are especially relevant in the modeling of elastic plates and related mechanical structures. Classical references such as Lagnese and Lions [2], Lagnese [3], and Lagnese, Leugering, and Schmidt [4] provide a fundamental basis for the analysis and control of thin plates and dynamic elastic systems. Compared with standard second-order diffusion or wave equations, fourth-order systems are more delicate because the biharmonic operator imposes stronger regularity requirements, more restrictive stability conditions, and a more careful treatment of boundary conditions.

Optimal control theory provides a rigorous framework for driving the state of a system toward a desired target while also taking into account the cost of the control. General tools for optimal control of PDEs can be found in the works of Li and Yong [5] and Tröltzsch [6], while the functional analytic background for boundary value problems is developed in Lions and Magenes [7] and Adams [8]. In the context of plate equations, several contributions have studied optimal control problems involving Kirchhoff and von Kármán plate models. Bradley and Lenhart [9] investigated bilinear optimal control of a Kirchhoff plate, and Bradley, Lenhart, and Yong [10] studied a related bilinear control problem involving the velocity term. Other works on plate models and optimal control include those of Prakash [11], Bock et al. [12], Park et al. [13], Hwang [14], Bradley [15], and Favini et al. [16].

Bilinear control problems form a particularly important class of optimal control problems. In contrast with purely additive controls, a bilinear control acts by modifying a coefficient, a transport mechanism, or a term multiplied by the state or by one of its derivatives. This type of control is useful in applications where the actuator changes an internal parameter of the system rather than simply adding an external force. In vibration and structural control, such mechanisms are related to active and semi-active control strategies, as discussed for example by Preumont [17] and Liu, Matsuhisa, and Utsuno [18]. These ideas are also related to vibration suppression and stiffness or damping modulation.

From a mathematical and numerical point of view, bilinear systems are more difficult than additive systems. Even when the state equation is linear for a fixed control, the dependence of the state on the control is generally nonlinear. As a consequence, the optimality system is nonlinear, and the computation of a descent direction or a step size becomes more delicate. In numerical algorithms, each evaluation of the cost functional may require solving the state equation again, which increases the computational cost. In addition, when the control appears in a transport-type term, numerical stability may become sensitive to the size of the control and to the time and space discretization. These difficulties are well known in bilinear advection-type control problems and require careful algorithmic design [19].

Several authors have studied bilinear control problems for wave, heat, parabolic, and plate equations. Zerrik and El Kabouss [20] considered regional optimal control of a bilinear wave equation, while Zerrik, Ait Aadi, and Ouhafsa [21] investigated a regional tracking problem for a bilinear wave equation with bounded controls. Ait Aadi and Zerrik [22] studied a constrained regional control problem for a bilinear plate equation. Boundary bilinear controls were considered by Lenhart and Wilson [23] and by Zerrik and El Kabouss [24, 25]. These works show that bilinear control is a natural and useful mechanism in many PDE models, but they also show that each class of equations requires a specific analysis.

Optimal control of wave equations has also been widely investigated. Liang [26] studied a bilinear optimal control problem for a wave equation. Kröner, Kunisch, and Vexler [27] developed semismooth Newton methods for wave equations with control constraints. Kunisch, Trautmann and Vexler [28] studied measure-valued controls for the undamped wave equation, while Gugat and Grimm [29] considered boundary control problems with pointwise constraints. Liu and Pearson [30] proposed parameter-robust preconditioning techniques for wave control problems. More recently, Clason, Kunisch, and Trautmann [31] studied the optimal control of the principal coefficient in a scalar wave equation. These contributions provide important tools and perspectives, but most of them concern second-order wave models rather than fourth-order dynamical systems. Second-order optimality analysis is another important aspect of PDE-constrained optimization. First-order conditions provide necessary information about an optimal control, but second-order conditions give a stronger characterization of local optimality and are important for stability and numerical optimization. Casas and Tröltzsch [32] studied second-order analysis for optimal control problems. Aronna and Tröltzsch [33] derived first- and second-order optimality conditions for Fokker–Planck equations, and El Mezegueldy, Yahyaoui, and Ouzahra [34] treated an infinite-horizon optimal control problem for a locally controlled Fokker–Planck equation. Other approaches have also been widely used for the control and stabilization of dynamical systems. Lyapunov-based methods are particularly useful for deriving stability conditions and constructing compensators, as illustrated for controlled engineering systems in [35]. Semigroup-based and decomposition approaches provide another powerful framework for the strong and exponential stabilization of semilinear systems in Banach spaces [36]. Compared with these stabilization-oriented techniques, the present work follows a PDE-constrained optimal control approach. Its main advantage is that it incorporates tracking objectives and control-energy minimization directly through the cost functional. However, the method is mainly formulated in a finite-horizon setting and requires solving both the state and adjoint systems.

However, for fourth-order dynamical systems with bilinear transport effects, the combination of well-posedness, optimal control existence, first-order characterization, second-order optimality conditions, and numerical validation remain less developed.

Motivated by observations in Table 1, the present paper studies a bilinear optimal control problem for a fourth-order evolution system. The model contains a biharmonic diffusion operator and a control action that affects the system through a transport-type term and a source contribution. This structure allows the control to influence both the spatial propagation of the state and its amplitude. The objective is to drive the state close to a prescribed desired profile while keeping the control energy small.

The first part of the paper is devoted to the analysis of the state system. We establish the well-posedness of the considered model and prove the existence of a solution under suitable assumptions. This step is essential because the optimal control problem is meaningful only if the state equation admits a well-defined solution for each admissible control. After that, we prove the existence of an optimal control by using the direct method of the calculus of variations. We then derive the associated adjoint system and characterize the optimal control through first-order optimality conditions. We also discuss second-order optimality conditions, which provide a stronger theoretical description of local optimal solutions.

The numerical part supports the theoretical results. A finite difference approximation is used for the state and adjoint systems, and an iterative descent algorithm is implemented to compute the control.

The numerical examples show a clear decrease of the distributed tracking error and the terminal tracking error. They also show that the control energy remains small during the optimization process. These results confirm the effectiveness of the proposed method and illustrate its ability to handle the additional difficulties generated by the fourth-order operator and the bilinear control term.

Table 1. Position of the present work with respect to related studies.

Reference	Fourth-order model	Bilinear advection control	Second-order conditions	Numerical gradient method
[9]	✓	×	×	×
[10]	✓	×	×	×
[22]	✓	×	×	×
[20]	×	✓	×	×
[21]	×	✓	×	×
[26]	×	✓	×	×
[31]	×	×	×	✓
[32]	×	×	✓	×
[33]	×	×	✓	×
Present paper	✓	✓	✓	✓

The main contributions of this paper, in connection with dynamical systems and mathematical control theory, are summarized as follows:

1. **Control of a fourth-order dynamical system.** We develop an optimal control framework for a second-order-in-time dynamical system governed by a fourth-order diffusion operator with advection effects.
2. **Bilinear control mechanism.** We study a drift-type bilinear control acting through the advection term. This provides a nonlinear control structure for distributed parameter systems described by differential equations.
3. **Well-posedness and existence.** We establish the well-posedness of the controlled state system and prove the existence of an optimal control by using the weak lower semicontinuity argument.
4. **Optimality system.** We derive the adjoint equation and the first-order optimality condition. We also discuss second-order necessary and sufficient conditions for local optimality.
5. **Numerical approximation.** We construct a finite difference scheme for the state and adjoint equations and combine it with a gradient-based algorithm to approximate the optimal control.
6. **Stability and performance analysis.** We discuss the influence of the main numerical parameters on stability, convergence, and tracking performance, which is directly related to the analysis of controlled dynamical systems.
7. **Numerical validation.** We present numerical simulations showing the reduction of distributed and terminal tracking errors while maintaining a small control energy.

The remainder of this paper is organized as follows. Section 2 introduces the controlled state system, specifies the functional framework, and establishes the well-posedness result. Section 3 formulates the optimal control problem, proves the weak lower semicontinuity of the cost functional, and establishes the existence of an optimal control. Section 4 derives the adjoint system and the first-order optimality condition. Section 5 presents the second-order necessary and sufficient optimality conditions. Section 6 describes the numerical discretization and the gradient-based algorithm. Section 7 presents the numerical simulations and discusses the stability indicators used to support the convergence of the scheme. Section 8 discusses the results, their interpretation, and their relation to existing studies. Finally, Section 9 concludes the paper.

2. The state system and well-posedness

In this section, we introduce the controlled fourth-order state system considered in this work. The model contains a biharmonic diffusion term and a bilinear advection control term. We specify the functional setting, the assumptions on the initial data and the admissible control, and the notion of weak solution. We then prove that, for every admissible control, the state equation admits a weak solution. This result is essential for the optimal control problem since the cost functional can be defined only when the state associated with each control is well determined. The proof is based on standard energy estimates.

Let Π be a bounded domain of $\mathbb{R}^n$ with $1 \leq n \leq 3$, and let $\partial\Pi$ be its boundary C^2. Choose $0 < T < +\infty$. The diffusion coefficient $\eta > 0$ and the reaction coefficient b_0 are assumed to be constant. In addition, we consider

$$h \in L^2(\Pi \times (0,T)), \qquad \phi_0 \in L^2(\Pi), \qquad \phi_1 \in L^2(\Pi).$$

We denote by

$$L^2_{\mathrm{div}}(\Pi) := \left\{ p \in L^2(\Pi)^n \ : \ \nabla \cdot p = 0 \text{ in the distributional sense in } \Pi \right\}.$$

Accordingly, we define the set of admissible controls as follows:

$$\mathcal{U}_{ad} = \left\{ p \in L^2(0,T; L^2_{\mathrm{div}}(\Pi)) \cap L^\infty(\Pi \times (0,T))^n \right\}, \tag{2.1}$$

The controlled system under consideration is given by

$$\begin{cases} \phi_{tt} + \eta\Delta^2\phi + p \cdot \nabla\phi = h & \text{in } \Pi \times (0,T), \\ \phi(\cdot,0) = \phi_0, \qquad \phi_t(\cdot,0) = \phi_1 & \text{in } \Pi, \\ \phi = 0, \qquad \dfrac{\partial\phi}{\partial\nu} = 0 & \text{on } \partial\Pi \times (0,T). \end{cases} \tag{2.2}$$

In system (2.2), the unknown function $\phi = \phi(x,t)$ denotes the state of the system, while $p = p(x,t)$ represents the bilinear control acting through the advection term. The constant $\eta > 0$ denotes the diffusion coefficient and $h = h(x,t)$ is a given source term. The functions ϕ_0 and ϕ_1 represent the initial position and the initial velocity, respectively. Finally, ϕ_0 and ϕ_1 are respectively the initial position and the initial velocity, and the condition $\phi = 0$ on $\partial\Pi \times (0,T)$ is a homogeneous Dirichlet boundary condition. This type of system arises in various problems where wave-like propagation, diffusion, and second-order time dynamics coexist. It can, for example, model a propagation phenomenon in a moving medium, in which advection describes the transport of the quantity under consideration, while diffusion represents its spatial spread [37, 38].

We start by establishing the results of existence, uniqueness, and regularity for the equation of state. To do this, we first introduce the functional framework

$$V = H_0^2(\Pi) = \left\{\phi \in H^2(\Pi)\ ;\ \phi = \frac{\partial \phi}{\partial \nu} = 0 \text{ on } \partial\Pi\right\},$$

and

$$H := V \times L^2(\Pi).$$

Next, we define the bilinear form $b : V \times V \to \mathbb{R}$ by

$$b(u, v) = \eta \int_\Pi \Delta u \, \Delta v \, dx.$$

It is well known that the form $b(\cdot, \cdot)$ is continuous and coercive on V, and that it induces on V a norm equivalent to the usual norm of $H^2(\Pi)$.

Definition 2.1. *Let $p \in \mathcal{U}_{ad}$ and $h \in L^2(\Pi \times (0, T))$. A function*

$$\tilde{\phi} = \tilde{\phi}(p) = (\phi(p), \phi_t(p))$$

is said to be the weak solution of system (2.2) if

$$\tilde{\phi} \in C([0, T]; H), \qquad \tilde{\phi}(0) = (\phi_0, \phi_1),$$

and if

$$\langle \phi_{tt}(t), \phi \rangle_{V',V} + b(\phi(t), \phi) + \int_\Pi (p(x, t) \cdot \nabla\phi(x, t))\, \phi(x)\, dx = \int_\Pi h(x, t)\phi(x)\, dx, \tag{2.3}$$

for all $\phi \in V$ and for almost all $t \in (0, T)$, where $\langle \cdot, \cdot \rangle_{V',V}$ denotes the duality bracket between V' and V.

The following theorem extends the classical existence and regularity results known for the Kirchhoff equation [6] to the fourth-order convective–diffusive equation, second order in time, considered in this work.

Theorem 2.1. *Let*

$$(\phi_0, \phi_1) \in H = V \times L^2(\Pi), \qquad h \in L^2(\Pi \times (0, T)), \qquad p \in \mathcal{U}_{ad}.$$

Then, system (2.2) admits a single weak solution $\tilde{\phi} = \tilde{\phi}(p) = (\phi, \phi_t)$, such as

$$\phi \in C([0, T]; V), \qquad \phi_t \in C([0, T]; L^2(\Pi)), \qquad \phi_{tt} \in L^2(0, T; V').$$

Moreover, if $(\phi_0, \phi_1) \in (H^4(\Pi) \cap V) \times V$, and if, in addition,

$$h \in H^1(0, T; L^2(\Pi)), \qquad p \in H^1(0, T; L^2(\Pi)^n) \cap \mathcal{U}_{ad},$$

then the weak solution admits the additional regularity

$$\phi \in C([0, T]; H^4(\Pi) \cap V), \qquad \phi_t \in C([0, T]; V), \qquad \phi_{tt} \in C([0, T]; L^2(\Pi)).$$

In particular, Eq (2.2) is satisfied in $L^2(\Pi)$ for almost all $t \in (0, T)$.

Proof. To write system (2.2) in an abstract evolution form, we first introduce the fourth-order elliptic operator

$$\mathcal{A}\phi = \eta\Delta^2\phi, \qquad D(\mathcal{A}) = H^4(\Pi) \cap H_0^2(\Pi).$$

This operator is the positive self-adjoint operator, associated with the bilinear form

$$a(u, v) = \eta \int_\Pi \Delta u \, \Delta v \, dx, \qquad u, v \in H_0^2(\Pi).$$

We then consider the energy space

$$\mathcal{H} = H_0^2(\Pi) \times L^2(\Pi),$$

endowed with the norm

$$\left\| \begin{pmatrix} \varphi_1 \\ \varphi_2 \end{pmatrix} \right\|_{\mathcal{H}}^2 = \|\Delta\varphi_1\|_{L^2(\Pi)}^2 + \|\varphi_2\|_{L^2(\Pi)}^2.$$

We define the matrix operator

$$\mathbb{A}\begin{pmatrix} \varphi_1 \\ \varphi_2 \end{pmatrix} = \begin{pmatrix} \varphi_2 \\ -\mathcal{A}\varphi_1 \end{pmatrix}, \qquad D(\mathbb{A}) = D(\mathcal{A}) \times H_0^2(\Pi).$$

Setting

$$\widetilde{\phi}(t) = \begin{pmatrix} \phi(t) \\ \phi_t(t) \end{pmatrix},$$

system (2.2) can be rewritten as

$$\frac{d}{dt}\widetilde{\phi}(t) = \mathbb{A}\widetilde{\phi}(t) + G(t, \widetilde{\phi}(t)), \qquad \widetilde{\phi}(0) = \begin{pmatrix} \phi_0 \\ \phi_1 \end{pmatrix}, \tag{2.4}$$

where

$$G(t, \widetilde{\phi}(t)) = \begin{pmatrix} 0 \\ h(t) - p(t) \cdot \nabla\phi(t) \end{pmatrix}.$$

Indeed, the first component of (2.4) gives

$$\frac{d}{dt}\phi(t) = \phi_t(t),$$

while the second component gives

$$\phi_{tt}(t) = -\mathcal{A}\phi(t) + h(t) - p(t) \cdot \nabla\phi(t).$$

Equivalently,

$$\phi_{tt}(t) + \mathcal{A}\phi(t) + p(t) \cdot \nabla\phi(t) = h(t),$$

which is precisely the abstract form of (2.2).

The convective term is understood in the weak sense. Since $p \in L^2(0, T; L^2(\Pi)^n)$ and $\operatorname{div} p = 0$, for every $v \in H_0^2(\Pi)$, we write

$$\int_\Pi (p \cdot \nabla\phi) v \, dx = -\int_\Pi \phi \, p \cdot \nabla v \, dx.$$

Using the Sobolev embedding $H_0^2(\Pi) \hookrightarrow L^\infty(\Pi)$, valid for $1 \le n \le 3$, we obtain

$$\left| \int_\Pi (p \cdot \nabla\phi) v \, dx \right| \le \|\phi\|_{L^\infty(\Pi)} \|p\|_{L^2(\Pi)^n} \|\nabla v\|_{L^2(\Pi)^n}.$$

Hence,

$$\left| \int_\Pi (p \cdot \nabla\phi) v \, dx \right| \le C \|p\|_{L^2(\Pi)^n} \|\phi\|_{H_0^2(\Pi)} \|v\|_{H_0^2(\Pi)}.$$

Therefore,

$$\|p \cdot \nabla\phi\|_{(H_0^2(\Pi))'} \le C \|p\|_{L^2(\Pi)^n} \|\phi\|_{H_0^2(\Pi)}.$$

Thus, the advection term is well defined as an element of $(H_0^2(\Pi))'$ and can be treated as a lower-order perturbation in the weak formulation.

Therefore, using classical semigroup arguments together with the energy estimates adapted to the transport term, we deduce that, for all initial conditions

$$(\phi_0, \phi_1) \in \mathcal{H},$$

system (2.2) admits a unique weak solution

$$\widetilde{\phi} \in C([0,T]; \mathcal{H}).$$

For the additional regularity result, assume that

$$\widetilde{\phi}_0 = (\phi_0, \phi_1) \in D(\mathbb{A}),$$

and that

$$h \in H^1(0,T; L^2(\Pi)), \qquad p \in H^1(0,T; L^2(\Pi)^n) \cap \mathcal{U}_{ad}.$$

By the variation-of-constants formula applied to (2.4), the weak solution satisfies

$$\widetilde{\phi}(t) = e^{t\mathbb{A}} \widetilde{\phi}_0 + \int_0^t e^{(t-s)\mathbb{A}} \begin{pmatrix} 0 \\ h(s) - p(s) \cdot \nabla\phi(s) \end{pmatrix} ds, \qquad t \in [0,T].$$

Differentiating this identity with respect to time and setting

$$\widetilde{\psi}(t) = \frac{d}{dt} \widetilde{\phi}(t) = \begin{pmatrix} \phi_t(t) \\ \phi_{tt}(t) \end{pmatrix},$$

we formally obtain

$$\widetilde{\psi}(t) = \mathbb{A} e^{t\mathbb{A}} \widetilde{\phi}_0 + \begin{pmatrix} 0 \\ h(t) - p(t) \cdot \nabla\phi(t) \end{pmatrix} + \int_0^t \mathbb{A} e^{(t-s)\mathbb{A}} \begin{pmatrix} 0 \\ h(s) - p(s) \cdot \nabla\phi(s) \end{pmatrix} ds.$$

By integrating by parts with respect to time, this relation can be rewritten as

$$\widetilde{\psi}(t) = \mathbb{A} e^{t\mathbb{A}} \widetilde{\phi}_0 + e^{t\mathbb{A}} \begin{pmatrix} 0 \\ h(0) - p(0) \cdot \nabla\phi_0 \end{pmatrix}$$

$$+\int_0^t e^{(t-s)\mathbb{A}}\begin{pmatrix}0\\ h_t(s)-p_t(s)\cdot\nabla\phi(s)-p(s)\cdot\nabla\phi_t(s)\end{pmatrix}ds. \tag{2.5}$$

This leads to the map L defined on $C([0,T_0];\mathcal{H})$, for $T_0>0$, by

$$\begin{aligned}L(\widetilde{\psi})(t)&=\mathbb{A}e^{t\mathbb{A}}\widetilde{\phi}_0+e^{t\mathbb{A}}\begin{pmatrix}0\\ h(0)-p(0)\cdot\nabla\phi_0\end{pmatrix}\\ &\quad+\int_0^t e^{(t-s)\mathbb{A}}\begin{pmatrix}0\\ h_t(s)-p_t(s)\cdot\nabla\phi(s)-p(s)\cdot\nabla\psi_1(s)\end{pmatrix}ds,\end{aligned} \tag{2.6}$$

where $\widetilde{\psi}=(\psi_1,\psi_2)$.

Since

$$\widetilde{\phi}_0\in D(\mathbb{A}),\qquad h\in H^1(0,T;L^2(\Pi)),\qquad p\in H^1(0,T;L^2(\Pi)^n)\cap\mathcal{U}_{ad},$$

the map L is well defined from $C([0,T_0];\mathcal{H})$ into itself. Moreover, for

$$\widetilde{\psi}^1=(\psi_1^1,\psi_2^1),\qquad \widetilde{\psi}^2=(\psi_1^2,\psi_2^2),$$

there exists a constant $C>0$, depending on p but independent of T_0, such that

$$\|L(\widetilde{\psi}^1)-L(\widetilde{\psi}^2)\|_{C([0,T_0];\mathcal{H})}\le CT_0\|\widetilde{\psi}^1-\widetilde{\psi}^2\|_{C([0,T_0];\mathcal{H})}.$$

Choosing $T_0>0$ sufficiently small so that $CT_0<1$, we deduce that L is a contraction on $C([0,T_0];\mathcal{H})$. Hence, by the Banach fixed point theorem, L admits a unique fixed point on $[0,T_0]$. Repeating the same argument on successive subintervals, we obtain

$$\widetilde{\psi}=(\phi_t,\phi_{tt})\in C([0,T];\mathcal{H}).$$

In particular,

$$\phi_t\in C([0,T];H_0^2(\Pi)),\qquad \phi_{tt}\in C([0,T];L^2(\Pi)).$$

Returning to Eq (2.2), we get

$$\mathcal{A}\phi=h-p\cdot\nabla\phi-\phi_{tt}.$$

Hence,

$$\Delta^2\phi\in C([0,T];L^2(\Pi)).$$

By standard elliptic regularity for the biharmonic operator with the homogeneous clamped boundary conditions

$$\phi=0,\qquad \frac{\partial\phi}{\partial\nu}=0\quad\text{on }\partial\Pi\times(0,T),$$

we obtain

$$\phi\in C([0,T];H^4(\Pi)\cap H_0^2(\Pi)).$$

Therefore,

$$\widetilde{\phi}\in C([0,T];(H^4(\Pi)\cap H_0^2(\Pi))\times H_0^2(\Pi)),\qquad \phi_{tt}\in C([0,T];L^2(\Pi)).$$

Thus, Eq (2.2) is satisfied in $L^2(\Pi)$ for almost every $t\in(0,T)$, which completes the proof. □

Lemma 2.1. *Assume that*

$$p \in \mathcal{U}_{ad}, \qquad h \in L^2(0, T; L^2(\Pi)),$$

and let

$$(\phi_0, \phi_1) \in H_0^2(\Pi) \times L^2(\Pi).$$

Then, the weak solution of (2.2) *satisfies the following energy estimate:*

$$\sup_{0 \le t \le T} \left(\|\phi_t(t)\|_{L^2(\Pi)}^2 + \eta \|\Delta\phi(t)\|_{L^2(\Pi)}^2 \right) \le C \left(\|\phi_1\|_{L^2(\Pi)}^2 + \eta \|\Delta\phi_0\|_{L^2(\Pi)}^2 + \|h\|_{L^2(0,T;L^2(\Pi))}^2 \right),$$

where $C > 0$ depends on T, η, Π, and $\|p\|_{L^\infty(\Pi\times(0,T))^n}$, but is independent of ϕ.

Proof. We assume, in this lemma, that

$$p \in \mathcal{U}_{ad} \cap L^\infty(\Pi \times (0, T))^n.$$

Multiplying Eq (2.2) by ϕ_t and integrating over Π, we obtain

$$\int_\Pi \phi_{tt}\phi_t \, dx + \eta \int_\Pi \Delta^2\phi \, \phi_t \, dx + \int_\Pi (p \cdot \nabla\phi)\phi_t \, dx = \int_\Pi h\phi_t \, dx.$$

Using

$$\int_\Pi \phi_{tt}\phi_t \, dx = \frac{1}{2}\frac{d}{dt}\|\phi_t\|_{L^2(\Pi)}^2,$$

and by Green's formula together with the homogeneous clamped boundary conditions,

$$\eta \int_\Pi \Delta^2\phi \, \phi_t \, dx = \frac{\eta}{2}\frac{d}{dt}\|\Delta\phi\|_{L^2(\Pi)}^2,$$

we deduce that

$$\frac{d}{dt}E(t) = \int_\Pi h\phi_t \, dx - \int_\Pi (p \cdot \nabla\phi)\phi_t \, dx,$$

where

$$E(t) = \frac{1}{2}\|\phi_t(t)\|_{L^2(\Pi)}^2 + \frac{\eta}{2}\|\Delta\phi(t)\|_{L^2(\Pi)}^2.$$

We now estimate the right-hand side. By the Cauchy–Schwarz and Young inequalities,

$$\left| \int_\Pi h\phi_t \, dx \right| \le \|h\|_{L^2(\Pi)}\|\phi_t\|_{L^2(\Pi)} \le \frac{1}{2}\|h\|_{L^2(\Pi)}^2 + \frac{1}{2}\|\phi_t\|_{L^2(\Pi)}^2.$$

Moreover, since $p \in L^\infty(\Pi \times (0, T))^n$, we have

$$\left| \int_\Pi (p \cdot \nabla\phi)\phi_t \, dx \right| \le \|p(t)\|_{L^\infty(\Pi)^n}\|\nabla\phi(t)\|_{L^2(\Pi)^n}\|\phi_t(t)\|_{L^2(\Pi)}.$$

By the Poincaré-type inequality on $H_0^2(\Pi)$, there exists a constant $C_\Pi > 0$ such that

$$\|\nabla\phi(t)\|_{L^2(\Pi)^n} \le C_\Pi \|\Delta\phi(t)\|_{L^2(\Pi)}.$$

Hence,

$$\left|\int_\Pi (p\cdot\nabla\phi)\phi_t\,dx\right| \le C_\Pi \|p(t)\|_{L^\infty(\Pi)^n}\|\Delta\phi(t)\|_{L^2(\Pi)}\|\phi_t(t)\|_{L^2(\Pi)}.$$

Using Young's inequality, we obtain

$$\left|\int_\Pi (p\cdot\nabla\phi)\phi_t\,dx\right| \le C\|p(t)\|^2_{L^\infty(\Pi)^n}\|\Delta\phi(t)\|^2_{L^2(\Pi)} + \frac{1}{2}\|\phi_t(t)\|^2_{L^2(\Pi)}.$$

Therefore,

$$\frac{d}{dt}E(t) \le C\left(1+\|p(t)\|^2_{L^\infty(\Pi)^n}\right)E(t) + \frac{1}{2}\|h(t)\|^2_{L^2(\Pi)}.$$

Since

$$\|p(t)\|_{L^\infty(\Pi)^n} \le \|p\|_{L^\infty(\Pi\times(0,T))^n},$$

we get

$$\frac{d}{dt}E(t) \le C_pE(t) + \frac{1}{2}\|h(t)\|^2_{L^2(\Pi)},$$

where

$$C_p = C\left(1+\|p\|^2_{L^\infty(\Pi\times(0,T))^n}\right).$$

By Gronwall's inequality, for every $t\in[0,T]$,

$$E(t) \le e^{C_pt}\left(E(0) + \frac{1}{2}\int_0^t \|h(s)\|^2_{L^2(\Pi)}\,ds\right).$$

Since

$$E(0) = \frac{1}{2}\|\phi_1\|^2_{L^2(\Pi)} + \frac{\eta}{2}\|\Delta\phi_0\|^2_{L^2(\Pi)},$$

we obtain

$$\sup_{0\le t\le T}\left(\|\phi_t(t)\|^2_{L^2(\Pi)} + \eta\|\Delta\phi(t)\|^2_{L^2(\Pi)}\right) \le C\left(\|\phi_1\|^2_{L^2(\Pi)} + \eta\|\Delta\phi_0\|^2_{L^2(\Pi)} + \|h\|^2_{L^2(0,T;L^2(\Pi))}\right),$$

where $C>0$ depends on T, η, Π, and $\|p\|_{L^\infty(\Pi\times(0,T))^n}$, but not on ϕ. Finally, integrating the preceding estimate in time gives

$$\eta\int_0^T \|\Delta\phi(s)\|^2_{L^2(\Pi)}\,ds \le CT\left(\|\phi_1\|^2_{L^2(\Pi)} + \eta\|\Delta\phi_0\|^2_{L^2(\Pi)} + \|h\|^2_{L^2(0,T;L^2(\Pi))}\right).$$

This proves the desired a priori estimate and completes the proof. □

Remark 2.1. *The additional assumption*

$$p\in L^\infty(\Pi\times(0,T))^n$$

is used only in Lemma 2.1 in order to derive the strong energy estimate by testing the equation with ϕ_t. Indeed, the estimate of the term

$$\int_\Pi (p\cdot\nabla\phi)\phi_t\,dx$$

requires the bound

$$\left|\int_{\Pi}(p\cdot\nabla\phi)\phi_t\,dx\right|\le\|p\|_{L^\infty(\Pi)^n}\|\nabla\phi\|_{L^2(\Pi)^n}\|\phi_t\|_{L^2(\Pi)}.$$

On the other hand, the weak formulation remains meaningful for $p\in\mathcal{U}_{ad}$ under the dimensional assumption $1\le n\le 3$, where the convective term can be interpreted by duality. Thus, the L^∞-assumption on p is not imposed on the whole admissible set, but only for the additional energy estimate stated in Lemma 2.1.

3. Problem formulation and existence of solution

In this section, we formulate the optimal control problem associated with the controlled state system introduced above. We first define the admissible control set and introduce the cost functional, which contains the tracking terms and the control penalization term. We then prove that the considered cost functional is weakly lower semicontinuous on the admissible control set. This property is a key ingredient in the existence analysis, since it allows us to pass to the limit along minimizing sequences. Finally, by using the direct method of the calculus of variations, together with the well-posedness and stability properties of the state equation, we prove that the optimal control problem admits at least one solution.

We consider the following bilinear optimal control problem:

$$\begin{cases}\boldsymbol{p}\in\mathcal{U}_{ad}\\ C(\boldsymbol{p})\le C(\boldsymbol{v}),\forall\boldsymbol{v}\in\mathcal{U}_{ad}\end{cases}\tag{3.1}$$

with the objective functional C defined by

$$C(\boldsymbol{p})=\frac{\sigma_1}{2}\iint_{\Pi\times(0;T)}|\phi-\phi_d|^2\,dxdt+\frac{\sigma_2}{2}\int_{\Pi}|\phi(T)-\phi_T|^2\,dx+\frac{1}{2}\iint_{\Pi\times(0;T)}|\boldsymbol{p}|^2dxdt,\tag{3.2}$$

where $\phi=\phi(t;\boldsymbol{p})$ is the solution of the advection-diffusion equation (2.2). The constants σ_1 and σ_2 are nonnegative constants, not both equal to zero, while the desired functions ϕ_d and ϕ_T are prescribed in $L^2(\Pi\times(0;T))$ and $L^2(\Pi)$, respectively. The cost functional (3.2) has a natural interpretation in real applications. Indeed, it aims to steer the state ϕ as close as possible to a desired trajectory ϕ_d over $\Pi\times(0,T)$ and to a prescribed terminal profile ϕ_T last time, while keeping the control effort p as small as possible. This formulation is particularly relevant in practical situations governed by bilinear hyperbolic systems, where one seeks to influence a propagation phenomenon efficiently under physical and operational constraints [12, 13].

Proposition 3.1. *The cost C, defined by* (3.2)*, is weakly lower semicontinuous on $\mathcal{U}_{ad}$. More precisely, let $\{p_m\}_{m\ge1}\subset\mathcal{U}_{ad}$ be a sequence such that $p_m\rightharpoonup p$ weakly in $\mathcal{U}_{ad}$. Then, one has*

$$C(p)\le\liminf_{m\to\infty}C(p_m).$$

Proof. Let $\{p_m\}_{m\ge1}$ be a sequence of controls such that

$$p_m\rightharpoonup p\quad\text{weakly in }L^2\Big(0,T;\boldsymbol{L}^2(\Pi)\Big).$$

For each $m \geq 1$, we denote $\phi_m = \phi(\cdot, \cdot; p_m)$ the state solution associated with p_m, i.e. the solution of

$$\phi_{m,tt} + \eta\Delta^2\phi_m + p_m \cdot \nabla\phi_m = h \quad \text{in } \Pi \times (0,T),$$

with the initial conditions

$$\phi_m(\cdot, 0) = \phi_0, \qquad \phi_{m,t}(\cdot, 0) = \phi_1 \quad \text{in } \Pi,$$

and the condition

$$\phi_m = 0, \qquad \frac{\partial \phi_m}{\partial \nu} = 0 \quad \text{on } \partial\Pi \times (0,T).$$

By the a priori estimates obtained for the state system, the sequence $\{\phi_m\}$ is bounded in the appropriate energy space. There is therefore a function ϕ such that, even if it means extracting a subsequence,

$$\phi_m \rightharpoonup \phi \quad \text{in the state space considered,}$$

and

$$\phi_{m,t} \rightharpoonup \phi_t \quad \text{in the corresponding space.}$$

In addition, thanks to an adapted weak compactness result [7], we also obtain a strong convergence of ϕ_m in an intermediate space, sufficient to process the bilinear term.

Now, let us move on to the limit in the weak formulation of the system. Linear terms are processed directly by weak convergence. For the transport term, the weak convergence of p_m combined with the strong convergence of ϕ_m allows us to write

$$\iint_{\Pi\times(0,T)} (p_m \cdot \nabla\phi_m)\, \psi \, dx\, dt \longrightarrow \iint_{\Pi\times(0,T)} (p \cdot \nabla\phi)\, \psi \, dx\, dt,$$

for any function $\psi \in V$. We deduce that ϕ satisfies the state system associated with the p control. By the uniqueness of the state solution, we then obtain

$$\phi = \phi(\cdot, \cdot; p).$$

Finally, by the weak lower semicontinuity of the norm in the control space, we obtain

$$\|p\|^2_{L^2(0,T;\boldsymbol{L}^2(\Pi))} \leq \liminf_{m\to\infty} \|p_m\|^2_{L^2(0,T;\boldsymbol{L}^2(\Pi))}.$$

Moreover, since $\phi_m \to \bar{\phi}$ strongly in $L^2(\Pi \times (0,T))$, we obtain

$$\iint_{\Pi\times(0,T)} |\phi_m - \phi_d|^2 \, dx\, dt \longrightarrow \iint_{\Pi\times(0,T)} |\bar{\phi} - \phi_d|^2 \, dx\, dt.$$

Moreover, the appropriate convergence of $\phi_m(T)$ to $\bar{\phi}(T)$ in $L^2(\Pi)$ results in

$$\int_{\Pi} |\bar{\phi}(T) - \phi_T|^2 \, dx \leq \liminf_{m\to\infty} \int_{\Pi} |\phi_m(T) - \phi_T|^2 \, dx.$$

By combining these three properties, we have

$$\begin{aligned}\liminf_{m\to\infty} C(\boldsymbol{p}_m) &= \liminf_{m\to\infty}\left[\frac{\sigma_1}{2}\iint_{\Pi\times(0,T)} |\phi_m-\phi_d|^2\,dx\,dt + \frac{\sigma_2}{2}\int_{\Pi} |\phi_m(T)-\phi_T|^2\,dx\right]\\ &+\left[\frac{1}{2}\iint_{\Pi\times(0,T)} |p_m|^2\,dx\,dt\right]\\ &\geq +\frac{\sigma_1}{2}\iint_{\Pi\times(0,T)} |\phi-\phi_d|^2\,dx\,dt + \frac{\sigma_2}{2}\int_{\Pi} |\phi(T)-\phi_T|^2\,dx + \frac{1}{2}\iint_{\Pi\times(0,T)} |p|^2\,dx\,dt\\ &= C(p).\end{aligned}$$

Combining this property with the convergences of the sequence of states, we obtain

$$C(p) \leq \liminf_{m\to\infty} C(p_m).$$

Thus, the cost functional C is weakly lower semicontinuous, which completes the proof. $\square$

Theorem 3.1. *The optimal control problem associated with the cost functional* (3.2) *admits at least one solution. More precisely, there exists a control $p \in \mathcal{U}_{ad}$ such that*

$$C(\boldsymbol{p}) = \min_{p\in\mathcal{U}_{ad}} C(p).$$

Equivalently, one has

$$C(p) \leq C(v), \qquad \forall\, v \in \mathcal{U}_{ad}.$$

Proof. Since the cost functional is nonnegative on the admissible set, the value

$$c = \inf_{p\in\mathcal{U}_{ad}} C(p)$$

is well defined. Therefore, there exists a minimizing sequence

$$(p_m)_{m\geq 1} \subset \mathcal{U}_{ad}$$

such that

$$\lim_{m\to\infty} C(p_m) = c.$$

From the definition of the cost functional, we deduce that the sequence (p_m) is bounded. More precisely, there exists a constant $M > 0$ such that

$$\|p_m\|_{L^2(0,T;L^2_{\mathrm{div}}(\Pi))} \leq M, \qquad \forall m.$$

Hence, (p_m) is bounded in the Hilbert space

$$L^2(0,T;L^2_{\mathrm{div}}(\Pi)).$$

Consequently, there exists a subsequence, still denoted by (p_m), and an element

$$p^* \in L^2(0,T;L^2_{\mathrm{div}}(\Pi))$$

such that

$$p_m \rightharpoonup p^* \quad \text{weakly in } L^2(0,T;L^2_{\text{div}}(\Pi)).$$

Since the admissible set $\mathcal{U}_{ad}$ is weakly closed, we obtain

$$p^* \in \mathcal{U}_{ad}.$$

Using the weak lower semicontinuity of C, we get

$$C(p^*) \leq \liminf_{m\to\infty} C(p_m) = c.$$

On the other hand, by the definition of c, we have

$$c \leq C(p^*).$$

Therefore,

$$C(p^*) = c = \inf_{p\in\mathcal{U}_{ad}} C(p),$$

which shows that p^* is an optimal control. □

4. First-order optimality condition

In this section, we derive the first-order optimality conditions associated with the bilinear control problem. The objective is to characterize the optimal control through a suitable optimality system involving the state and an adjoint variable. We first compute the first-order derivative of the reduced cost functional with respect to the control variable. This is achieved by means of a perturbation argument combined with a linearization of the state equation. The introduction of an adjoint system allows us to eliminate the dependence on the state variation and to obtain an explicit expression of the gradient of the cost functional.

The resulting optimality conditions provide a necessary condition for optimality and lead to a coupled system consisting of the state equation, the adjoint equation, and a variational relation that characterizes the optimal control.

Proposition 4.1. *Let $p \in \mathcal{U}_{ad}$, and let ϕ be the corresponding solution of the state system* (2.2). *Assume that the reduced cost functional is given by*

$$C(p) = \frac{\alpha_1}{2}\iint_{\Pi\times(0,T)} |\phi-\phi_d|^2\,dxdt + \frac{\alpha_2}{2}\int_{\Pi}|\phi(T)-\phi_T|^2\,dx + \frac{1}{2}\iint_{\Pi\times(0,T)}|p|^2\,dxdt.$$

Then, the first-order derivative of C at p is given by

$$C'(p) = p - \psi\nabla\phi,$$

where ψ is the solution of the adjoint system

$$\begin{cases} \psi_{tt} + \eta\Delta^2\psi - p\cdot\nabla\psi = \alpha_1(\phi-\phi_d) & \text{in } \Pi\times(0,T),\\ \psi(\cdot,T) = \alpha_2(\phi(T)-\phi_T), \qquad \psi_t(\cdot,T) = 0 & \text{in } \Pi,\\ \psi = 0, \qquad \dfrac{\partial\psi}{\partial\nu} = 0 & \text{on } \partial\Pi\times(0,T). \end{cases}$$

Equivalently, for every admissible perturbation δp, one has

$$\delta C(p) = \iint_{\Pi\times(0,T)} (p - \psi\nabla\phi)\cdot\delta p\,dxdt.$$

Proof. Let δp be an admissible perturbation of p, and denote by $\delta\phi$ the corresponding variation of the state. Linearizing the state equation with respect to the control gives

$$\begin{cases} \delta\phi_{tt} + \eta\Delta^2\delta\phi + p\cdot\nabla\delta\phi + \delta p\cdot\nabla\phi = 0 & \text{in } \Pi\times(0,T),\\ \delta\phi(\cdot,0) = 0, \qquad \delta\phi_t(\cdot,0) = 0 & \text{in } \Pi,\\ \delta\phi = 0, \qquad \dfrac{\partial\delta\phi}{\partial\nu} = 0 & \text{on } \partial\Pi\times(0,T). \end{cases}$$

By differentiating the cost functional in the direction δp, we obtain

$$\delta C(p) = \iint_{\Pi\times(0,T)} p\cdot\delta p\,dxdt + \alpha_1\iint_{\Pi\times(0,T)}(\phi-\phi_d)\delta\phi\,dxdt + \alpha_2\int_\Pi(\phi(T)-\phi_T)\delta\phi(T)\,dx.$$

We now introduce the adjoint variable ψ as the solution of

$$\begin{cases} \psi_{tt} + \eta\Delta^2\psi - p\cdot\nabla\psi = \alpha_1(\phi-\phi_d) & \text{in } \Pi\times(0,T),\\ \psi(\cdot,T) = \alpha_2(\phi(T)-\phi_T), \qquad \psi_t(\cdot,T) = 0 & \text{in } \Pi,\\ \psi = 0, \qquad \dfrac{\partial\psi}{\partial\nu} = 0 & \text{on } \partial\Pi\times(0,T). \end{cases}$$

Multiplying the linearized equation by ψ, integrating over $\Pi\times(0,T)$, and applying integration by parts in time together with Green's formula for the biharmonic operator, we get

$$\alpha_1\iint_{\Pi\times(0,T)}(\phi-\phi_d)\delta\phi\,dxdt + \alpha_2\int_\Pi(\phi(T)-\phi_T)\delta\phi(T)\,dx = -\iint_{\Pi\times(0,T)}\psi\,\delta p\cdot\nabla\phi\,dxdt.$$

More precisely, starting from the linearized equation

$$\delta\phi_{tt} + \eta\Delta^2\delta\phi + p\cdot\nabla\delta\phi + \delta p\cdot\nabla\phi = 0,$$

we multiply by the adjoint variable ψ and integrate over $\Pi\times(0,T)$. For the time derivative, using

$$\delta\phi(.,0) = 0, \qquad \delta\phi_t(.,0) = 0,$$

and the terminal conditions

$$\psi(T) = \alpha_2(\phi(T)-\phi_T), \qquad \psi_t(T) = 0,$$

we obtain

$$\int_0^T\int_\Pi\delta\phi_{tt}\psi\,dxdt = \int_0^T\int_\Pi\delta\phi\,\psi_{tt}\,dxdt + \alpha_2\int_\Pi(\phi(T)-\phi_T)\delta\phi(T)\,dx.$$

For the fourth-order term, Green's formula for the biharmonic operator gives

$$\int_0^T\int_\Pi\Delta^2\delta\phi\,\psi\,dxdt = \int_0^T\int_\Pi\delta\phi\,\Delta^2\psi\,dxdt,$$

because the clamped boundary conditions

$$\delta\phi = \frac{\partial \delta\phi}{\partial \nu} = 0, \qquad \psi = \frac{\partial \psi}{\partial \nu} = 0 \quad \text{on } \partial\Pi \times (0, T)$$

make all boundary terms vanish. For the advection term, using the divergence-free condition

$$\operatorname{div} p = 0,$$

and the boundary condition $\delta\phi(., 0) = 0$ on $\partial\Pi \times (0, T)$, we have

$$\int_\Pi (p \cdot \nabla \delta\phi)\psi \, dx = - \int_\Pi \delta\phi \, p \cdot \nabla \psi \, dx.$$

Indeed,

$$\int_\Pi (p \cdot \nabla \delta\phi)\psi \, dx = - \int_\Pi \delta\phi \, \operatorname{div}(p\psi) \, dx + \int_{\partial\Pi} \delta\phi \, \psi \, p \cdot \nu \, d\sigma,$$

and the boundary integral is zero since $\delta\phi(., 0) = 0$ on $\partial\Pi$, while

$$\operatorname{div}(p\psi) = p \cdot \nabla\psi + \psi \, \operatorname{div} p = p \cdot \nabla\psi.$$

Therefore,

$$\int_\Pi (p \cdot \nabla \delta\phi)\psi \, dx = - \int_\Pi \delta\phi \, p \cdot \nabla \psi \, dx.$$

Combining these identities gives the adjoint equation

$$\psi_{tt} + \eta\Delta^2\psi - p \cdot \nabla\psi = \alpha_1(\phi - \phi_d) \quad \text{in } \Pi \times (0, T),$$

with the terminal and boundary conditions stated in the manuscript. Consequently, the terms containing $\delta\phi$ are eliminated and we obtain

$$\delta C(p) = \int_0^T \int_\Pi (p - \psi\nabla\phi) \cdot \delta p \, dxdt.$$

Thus,

$$C'(p) = p - \psi\nabla\phi.$$

The proof is complete.

□

Theorem 4.1. *Let $p^* \in \mathcal{U}_{ad}$ be an optimal control for the problem associated with the state system* (2.2). *Then, p^* satisfies the following first-order optimality condition:*

$$\iint_{\Pi\times(0,T)} (p^* - \psi\nabla\phi) \cdot (v - p^*) \, dxdt \geq 0, \qquad \forall v \in \mathcal{U}_{ad},$$

where ϕ is the state associated with p^*, and ψ is the solution of the adjoint system

$$\begin{cases} \psi_{tt} + \eta\Delta^2\psi - p^* \cdot \nabla\psi = \alpha_1(\phi - \phi_d) & \text{in } \Pi \times (0, T), \\ \psi(\cdot, T) = \alpha_2(\phi(T) - \phi_T), \qquad \psi_t(\cdot, T) = 0 & \text{in } \Pi, \\ \psi = 0, \qquad \dfrac{\partial\psi}{\partial\nu} = 0 & \text{on } \partial\Pi \times (0, T). \end{cases} \tag{4.1}$$

Proof. Let $p^* \in \mathcal{U}_{ad}$ be an optimal control. Since $\mathcal{U}_{ad}$ is convex, for every $v \in \mathcal{U}_{ad}$ and every $\varepsilon \in (0, 1)$, the control

$$p_\varepsilon = p^* + \varepsilon(v - p^*)$$

belongs to $\mathcal{U}_{ad}$. By the optimality of p^*, we have

$$C(p_\varepsilon) - C(p^*) \geq 0.$$

Dividing by ε gives

$$\frac{C(p^* + \varepsilon(v - p^*)) - C(p^*)}{\varepsilon} \geq 0.$$

Passing to the limit as $\varepsilon \to 0^+$, we obtain

$$C'(p^*)(v - p^*) \geq 0.$$

Using the expression of the derivative of C, namely

$$C'(p^*)z = \iint_{\Pi\times(0,T)} (p^* - \psi\nabla\phi) \cdot z\, dxdt,$$

with $z = v - p^*$, we deduce

$$\iint_{\Pi\times(0,T)} (p^* - \psi\nabla\phi) \cdot (v - p^*)\, dxdt \geq 0, \qquad \forall v \in \mathcal{U}_{ad}. \tag{4.2}$$

This proves the desired optimality condition. □

5. Second-order optimality conditions

In this section, we complete the optimality analysis by studying the second-order behavior of the cost functional. After deriving the first-order optimality system, we introduce the second derivative of the reduced cost functional with respect to the control variable. We then use this second derivative to state the second-order necessary optimality condition satisfied by a local optimal control. This condition provides additional information beyond the first-order condition and is useful for analyzing the local behavior of the cost functional around an optimal control. Finally, we present a second-order sufficient optimality condition. This condition guarantees that a feasible control satisfying the first-order condition is indeed a strict local minimizer, provided that the second variation is positive on the appropriate critical directions.

Proposition 5.1. *The reduced cost functional $C : \mathcal{U}_{ad} \to \mathbb{R}$ is Fréchet differentiable twice continuously.*

Let $p \in \mathcal{U}_{ad}$, and let ϕ and ψ be the associated state and adjoint variables. For any directions $h_1, h_2 \in \mathcal{U}_{ad}$, the second derivative of C is given by

$$\begin{aligned} C''(p)[h_1, h_2] = &\int_{\Pi\times(0,T)} h_1 \cdot h_2\, dxdt + \alpha_1 \int_{\Pi\times(0,T)} z_1 z_2\, dxdt + \alpha_2 \int_\Pi z_1(T) z_2(T)\, dx \\ &- \int_{\Pi\times(0,T)} \psi(h_1 \cdot \nabla z_2 + h_2 \cdot \nabla z_1)\, dxdt. \end{aligned} \tag{5.1}$$

where z_i denotes the solution of the linearized state equation corresponding to direction h_i, that is,

$$\begin{cases} z_{i,tt} + \eta\Delta^2 z_i + p\cdot\nabla z_i + h_i\cdot\nabla\phi = 0 & \text{in } \Pi\times(0,T), \\ z_i(\cdot,0) = 0, \quad z_{i,t}(\cdot,0) = 0 & \text{in } \Pi, \\ z_i = 0, \quad \dfrac{\partial z_i}{\partial\nu} = 0 & \text{on } \partial\Pi\times(0,T). \end{cases} \tag{5.2}$$

Proof. Let $h_1, h_2 \in \mathcal{U}_{ad}$. For $S : p \mapsto \phi(p)$, and $i = 1,2$, we denote by $z_i = S'(p)h_i$ the first variation of the state in the direction h_i. Then, z_i satisfies

$$\begin{cases} z_{i,tt} + \eta\Delta^2 z_i + p\cdot\nabla z_i + h_i\cdot\nabla\phi = 0 & \text{in } \Pi\times(0,T), \\ z_i(\cdot,0) = 0, \qquad z_{i,t}(\cdot,0) = 0 & \text{in } \Pi, \\ z_i = 0, \qquad \dfrac{\partial z_i}{\partial\nu} = 0 & \text{on } \partial\Pi\times(0,T). \end{cases}$$

We also denote by

$$\zeta = S''(p)[h_1,h_2]$$

the second variation of the state. Differentiating the linearized equation once more gives

$$\begin{cases} \zeta_{tt} + \eta\Delta^2\zeta + p\cdot\nabla\zeta + h_1\cdot\nabla z_2 + h_2\cdot\nabla z_1 = 0 & \text{in } \Pi\times(0,T), \\ \zeta(\cdot,0) = 0, \qquad \zeta_t(\cdot,0) = 0 & \text{in } \Pi, \\ \zeta = 0, \qquad \dfrac{\partial\zeta}{\partial\nu} = 0 & \text{on } \partial\Pi\times(0,T). \end{cases}$$

By differentiating the cost functional twice, we obtain

$$\begin{aligned} C''(p)[h_1,h_2] = &\iint_{\Pi\times(0,T)} h_1\cdot h_2\,dxdt + \alpha_1\iint_{\Pi\times(0,T)} z_1 z_2\,dxdt \\ &+ \alpha_1\iint_{\Pi\times(0,T)} (\phi-\phi_d)\zeta\,dxdt + \alpha_2\int_\Pi z_1(T)z_2(T)\,dx \\ &+ \alpha_2\int_\Pi (\phi(T)-\phi_T)\zeta(T)\,dx. \end{aligned}$$

We now use the adjoint equation in order to eliminate the terms containing ζ. Recall that ψ satisfies

$$\begin{cases} \psi_{tt} + \eta\Delta^2\psi - p\cdot\nabla\psi = \alpha_1(\phi-\phi_d) & \text{in } \Pi\times(0,T), \\ \psi(\cdot,T) = \alpha_2(\phi(T)-\phi_T), \qquad \psi_t(\cdot,T) = 0 & \text{in } \Pi, \\ \psi = 0, \qquad \dfrac{\partial\psi}{\partial\nu} = 0 & \text{on } \partial\Pi\times(0,T). \end{cases}$$

Multiplying the equation satisfied by ζ by ψ, integrating over $\Pi\times(0,T)$, and using integration by parts in time together with Green's formula for the biharmonic operator, we obtain

$$\begin{aligned} \alpha_1 &\iint_{\Pi\times(0,T)} (\phi-\phi_d)\zeta\,dxdt + \alpha_2\int_\Pi (\phi(T)-\phi_T)\zeta(T)\,dx \\ &= -\iint_{\Pi\times(0,T)} \psi\,(h_1\cdot\nabla z_2 + h_2\cdot\nabla z_1)\,dxdt. \end{aligned}$$

Substituting this identity into the expression of $C''(p)[h_1, h_2]$, we get

$$\begin{aligned} C''(p)[h_1, h_2] = &\iint_{\Pi\times(0,T)} h_1 \cdot h_2 \, dxdt + \alpha_1 \iint_{\Pi\times(0,T)} z_1 z_2 \, dxdt \\ &+ \alpha_2 \int_{\Pi} z_1(T) z_2(T) \, dx \\ &- \iint_{\Pi\times(0,T)} \psi \left(h_1 \cdot \nabla z_2 + h_2 \cdot \nabla z_1\right) \, dxdt. \end{aligned}$$

This proves the stated expression of the second derivative. □

Definition 5.1. *Let $p^* \in \mathcal{U}_{ad}$ be an optimal control. The critical cone at p^* is defined by*

$$C(p^*) = \{h \in \mathcal{U}_{ad} \ : \ C'(p^*)[h] = 0\}.$$

Theorem 5.1. *Let $p^* \in \mathcal{U}_{ad}$ be a local optimal control, and assume that the reduced cost functional C is twice Fréchet differentiable in a neighborhood of p^*. Then,*

$$C''(p^*)[h, h] \geq 0, \qquad \forall h \in C(p^*),$$

where

$$C(p^*) = \{h \in \mathcal{U}_{ad} \ : \ C'(p^*)[h] = 0\}.$$

Proof. Let $h \in C(p^*)$. Since p^* is a local minimizer, for every sufficiently small $\varepsilon > 0$, we have

$$C(p^*) \leq C(p^* + \varepsilon h).$$

Using Taylor's expansion of C at p^* in the direction h, we obtain

$$C(p^* + \varepsilon h) = C(p^*) + \varepsilon C'(p^*)[h] + \frac{\varepsilon^2}{2} C''(p^*)[h, h] + o(\varepsilon^2).$$

Since $h \in C(p^*)$, one has

$$C'(p^*)[h] = 0.$$

Therefore,

$$0 \leq C(p^* + \varepsilon h) - C(p^*) = \frac{\varepsilon^2}{2} C''(p^*)[h, h] + o(\varepsilon^2).$$

Dividing by $\varepsilon^2/2$, we get

$$0 \leq C''(p^*)[h, h] + o(1).$$

Passing to the limit as $\varepsilon \to 0^+$, we obtain

$$C''(p^*)[h, h] \geq 0.$$

This completes the proof. □

Theorem 5.2. *Let $p^* \in \mathcal{U}_{ad}$ satisfy the first-order optimality condition*

$$C'(p^*)[h] = 0, \qquad \forall h \in \mathcal{U}_{ad}.$$

Assume that there exists a constant $\mu > 0$ such that

$$C''(p^*)[h,h] \geq \mu \|h\|^2_{L^2(0,T;L^2(\Pi)^n)}, \qquad \forall h \in C(p^*).$$

Then, p^* is a strict local optimal control. More precisely, there exist constants $\rho > 0$ and $\delta > 0$ such that

$$C(p) \geq C(p^*) + \delta \|p - p^*\|^2_{L^2(0,T;L^2(\Pi)^n)}$$

for every $p \in \mathcal{U}_{ad}$ satisfying

$$\|p - p^*\|_{L^2(0,T;L^2(\Pi)^n)} \leq \rho.$$

Proof. Let $p \in \mathcal{U}_{ad}$ be sufficiently close to p^*, and set

$$h = p - p^*.$$

By Taylor's formula, we have

$$C(p) = C(p^*) + C'(p^*)[h] + \frac{1}{2} C''(p^*)[h,h] + o\left(\|h\|^2_{L^2(0,T;L^2(\Pi)^n)}\right).$$

Since p^* satisfies the first-order optimality condition, we have

$$C'(p^*)[h] = 0.$$

Thus,

$$C(p) - C(p^*) = \frac{1}{2} C''(p^*)[h,h] + o\left(\|h\|^2_{L^2(0,T;L^2(\Pi)^n)}\right).$$

Using the coercivity assumption, we obtain

$$C(p) - C(p^*) \geq \frac{\mu}{2} \|h\|^2_{L^2(0,T;L^2(\Pi)^n)} + o\left(\|h\|^2_{L^2(0,T;L^2(\Pi)^n)}\right).$$

For p sufficiently close to p^*, the remainder term satisfies

$$\left| o\left(\|h\|^2_{L^2(0,T;L^2(\Pi)^n)}\right) \right| \leq \frac{\mu}{4} \|h\|^2_{L^2(0,T;L^2(\Pi)^n)}.$$

Therefore,

$$C(p) - C(p^*) \geq \frac{\mu}{4} \|h\|^2_{L^2(0,T;L^2(\Pi)^n)}.$$

Taking $\delta = \mu/4$, we obtain

$$C(p) \geq C(p^*) + \delta \|p - p^*\|^2_{L^2(0,T;L^2(\Pi)^n)}.$$

Hence, p^* satisfies the quadratic growth condition and is therefore a strict local optimal control. □

6. Numerical approach

In this section, we present a numerical method to approximate the optimal control and the corresponding state. Since the optimality system is nonlinear and coupled, it cannot be solved analytically in general. We discretize the state and adjoint equations in space and time using a finite difference scheme. Then, we solve the resulting optimality system by an iterative method based on the gradient of the cost functional. At each iteration, the state equation and the adjoint equation are solved successively and the control is updated using the computed gradient. The iteration is stopped when a suitable convergence criterion is satisfied. This approach allows us to compute an approximation of the optimal control and to illustrate the theoretical results through numerical simulations.

6.1. Finite difference approximation

For simplicity, we consider the one-dimensional case $\Pi = (0, L)$. In this case, the divergence-free condition imposed on the control reduces to

$$\operatorname{div} p = 0 \quad \Longleftrightarrow \quad p_x = 0.$$

Therefore, in order to respect the admissibility condition and to simplify the numerical computation, we take the control in the form $p = p(t)$. Consequently, at the discrete level, the same value of the control is used at all spatial grid points:

$$p_i^n = p^n, \qquad i = 0, \ldots, N.$$

We discretize the interval $(0, L)$ by

$$x_i = i\Delta x, \qquad i = 0, 1, \ldots, N, \qquad \Delta x = \frac{L}{N}.$$

The time interval $(0, T)$ is discretized by

$$t^n = n\Delta t, \qquad n = 0, 1, \ldots, M, \qquad \Delta t = \frac{T}{M}.$$

We denote

$$\phi_i^n \approx \phi(x_i, t^n), \qquad p^n \approx p(t^n), \qquad h_i^n \approx h(x_i, t^n).$$

The finite difference scheme of the state system is

$$\frac{\phi_i^{n+1} - 2\phi_i^n + \phi_i^{n-1}}{(\Delta t)^2} + \eta \frac{\phi_{i-2}^n - 4\phi_{i-1}^n + 6\phi_i^n - 4\phi_{i+1}^n + \phi_{i+2}^n}{(\Delta x)^4} + p^n \frac{\phi_{i+1}^n - \phi_{i-1}^n}{2\Delta x} = h_i^n. \tag{6.1}$$

Equivalently, the explicit update formula is

$$\begin{aligned} \phi_i^{n+1} = 2\phi_i^n - \phi_i^{n-1} + (\Delta t)^2 \Bigg[h_i^n - \eta \frac{\phi_{i-2}^n - 4\phi_{i-1}^n + 6\phi_i^n - 4\phi_{i+1}^n + \phi_{i+2}^n}{(\Delta x)^4} \\ - p^n \frac{\phi_{i+1}^n - \phi_{i-1}^n}{2\Delta x} \Bigg], \end{aligned} \tag{6.2}$$

with

$$\phi_i^0 = \phi_0(x_i), \qquad \phi_i^1 = \phi_1(x_i).$$

The clamped boundary conditions are

$$\phi_0^n = 0, \qquad \phi_N^n = 0,$$

and

$$\phi_{-1}^n = \phi_1^n, \qquad \phi_{N+1}^n = \phi_{N-1}^n.$$

For the adjoint equation, the finite difference scheme is

$$\frac{\psi_i^{n+1} - 2\psi_i^n + \psi_i^{n-1}}{(\Delta t)^2} + \eta\frac{\psi_{i-2}^n - 4\psi_{i-1}^n + 6\psi_i^n - 4\psi_{i+1}^n + \psi_{i+2}^n}{(\Delta x)^4} - p^n\frac{\psi_{i+1}^n - \psi_{i-1}^n}{2\Delta x} = \alpha_1(\phi_i^n - \phi_{d,i}^n). \tag{6.3}$$

Since the adjoint equation is solved backward in time, we write the update formula for ψ_i^{n-1} as

$$\begin{aligned}\psi_i^{n-1} = 2\psi_i^n - \psi_i^{n+1} + (\Delta t)^2\Bigg[&\alpha_1(\phi_i^n - \phi_{d,i}^n) - \eta\frac{\psi_{i-2}^n - 4\psi_{i-1}^n + 6\psi_i^n - 4\psi_{i+1}^n + \psi_{i+2}^n}{(\Delta x)^4} \\ &+ p^n\frac{\psi_{i+1}^n - \psi_{i-1}^n}{2\Delta x}\Bigg].\end{aligned} \tag{6.4}$$

The terminal conditions for the adjoint are

$$\psi_i^M = \alpha_2(\phi_i^M - \phi_{T,i}), \qquad \psi_i^{M+1} = \psi_i^M.$$

The boundary conditions for the adjoint are

$$\psi_0^n = 0, \qquad \psi_N^n = 0,$$

and

$$\psi_{-1}^n = \psi_1^n, \qquad \psi_{N+1}^n = \psi_{N-1}^n.$$

Remark 6.1. *The notation p^n is used in the one-dimensional simulations because the divergence-free condition implies that the control is independent of the space variable. Hence, the discrete divergence-free condition is satisfied exactly:*

$$\frac{p_{i+1}^n - p_{i-1}^n}{2\Delta x} = 0.$$

Therefore, no spatial update of the control is performed in the reported one-dimensional experiments; at each time level, the same value p^n is used for all spatial grid points. This clarification makes the numerical scheme consistent with the theoretical admissible set.

6.2. Gradient-based descent algorithm with backtracking step size

We now describe the iterative gradient-based algorithm used to approximate the optimal control. At each iteration, the state equation is solved forward in time, the adjoint equation is solved backward in time, and the control is updated in the negative gradient direction.

Initialization. Choose an initial control p^0, an initial step size $\tau^0 > 0$, a reduction factor $\theta \in (0, 1)$, and a tolerance $\varepsilon > 0$. Set $k = 0$.

Step 1: State equation. Solve the state system with the control p^k to obtain the state ϕ^k.

Step 2: Adjoint equation. Solve the adjoint system backward in time using ϕ^k and p^k to obtain the adjoint state ψ^k.

Step 3: Gradient computation. Compute the gradient of the reduced cost functional:

$$g^k = C'(p^k) = p^k - \psi^k \nabla \phi^k.$$

Step 4: Step-size selection. Set $\tau_k = \tau^0$. If the trial control

$$\widetilde{p}^k = p^k - \tau_k g^k$$

does not decrease the cost functional, reduce the step size according to

$$\tau_k \leftarrow \theta \tau_k,$$

and repeat this procedure until a decrease of the cost functional is obtained.

Step 5: Control update. Update the control by

$$p^{k+1} = p^k - \tau_k g^k.$$

Step 6: Stopping criterion. If

$$\|g^k\|_{L^2(0,T;L^2(\Pi)^n)} \leq \varepsilon,$$

or if the maximum number of iterations is reached, stop. Otherwise, set $k \leftarrow k + 1$ and return to Step 1.

Remark 6.2.

1. *At each iteration, the algorithm requires solving one state equation and one adjoint equation. The convergence depends on the choice of the step size and the stopping criterion.*
2. *The following quantities are used as practical stability indicators:*

$$C_{\text{bih}} = 16\,\eta\,\frac{(\Delta t)^2}{(\Delta x)^4}, \qquad C_\lambda = |\lambda|(\Delta t)^2, \qquad C_{\text{adv}} = p_{\max}\frac{\Delta t}{\Delta x}.$$

3. *The quantity $C_\lambda = |\lambda|(\Delta t)^2$ is motivated by the classical root stability condition of the leapfrog scheme applied to*

$$u_{tt} + \lambda u = 0.$$

   For this scalar equation, stability requires

$$0 \leq \lambda(\Delta t)^2 \leq 4.$$

4. *The quantity C_{bih} comes from the discrete fourth-order operator. The largest Fourier symbol of the discrete biharmonic operator is*

$$\frac{16}{(\Delta x)^4}.$$

   Hence,

$$C_{\text{bih}} = 16\eta\frac{(\Delta t)^2}{(\Delta x)^4}.$$

5. *The combined condition*
$$C_{\text{bih}} + C_\lambda < 4$$
is used as a practical CFL-type indicator for the explicit treatment of the biharmonic and source/reaction terms. The advection contribution is monitored separately through
$$C_{\text{adv}} < 1.$$
6. *These restrictions are practical indicators motivated by the classical von Neumann stability analysis for explicit finite difference schemes; see, for example, LeVeque [39]. They are not claimed to constitute a complete stability theorem for the full controlled system.*

7. Simulation results

In this section, we present numerical simulations illustrating the performance of the proposed optimal control strategy. Two numerical examples are considered in order to test the effectiveness of the method for different target profiles and parameter choices. The aim is to show how the controlled state approaches the prescribed target and to analyze the evolution of the distributed error, the terminal error, and the control energy during the iterative process.

Before presenting the simulations, we discuss the practical stability indicators of the finite difference scheme. This step is important because the presence of the fourth-order diffusion term and the bilinear advection control may impose restrictive conditions on the time and space discretization. The numerical parameters are therefore selected so as to preserve the stability of the scheme and to support the convergence of the gradient-based algorithm. For simplicity and clarity, the computations are carried out on the one-dimensional spatial domain $\Pi = (0, 1)$ over the time interval $(0, T)$. In accordance with the one-dimensional divergence-free constraint, the control is implemented as a time-dependent scalar $p = p(t)$.

The source term is chosen as $h(x, t) = \lambda\phi(x, t)$. The initial conditions are given by
$$\phi(x, 0) = \phi_0(x), \qquad \phi_t(x, 0) = \phi_1(x),$$
where, for instance,
$$\phi_0(x) = x^2(1 - x)^2, \qquad \phi_1(x) = 0,$$
The boundary conditions are
$$\phi(0, t) = \phi(1, t) = 0, \qquad \phi_x(0, t) = \phi_x(1, t) = 0.$$
The problem is discretized using a finite difference scheme in space and time. The gradient descent algorithm is then applied to the discrete optimality system. At each iteration, the state equation is solved forward in time, the adjoint equation is solved backward in time, and the control is updated using the computed gradient.

The stopping criterion for the gradient descent algorithm is defined by
$$\|g^k\| \leq \varepsilon,$$
where the tolerance is fixed as ε, and the maximum number of iterations is denoted by $K_{\max}$.

In addition to the stopping criterion, we monitor the evolution of the cost functional and the accuracy of the state with respect to the desired targets.

At each iteration k, the value of the cost functional is computed as

$$C(p^k) = \frac{\alpha_1}{2} \iint_{\Pi\times(0,T)} |\phi^k - \phi_d|^2 \, dxdt + \frac{\alpha_2}{2} \int_{\Pi} |\phi^k(T) - \phi_T|^2 \, dx + \frac{1}{2} \iint_{\Pi\times(0,T)} |p^k|^2 \, dxdt.$$

We also evaluate the tracking errors

$$E_1^k = \|\phi^k - \phi_d\|^2_{L^2(\Pi\times(0,T))}, \qquad E_2^k = \|\phi^k(T) - \phi_T\|^2_{L^2(\Pi)}.$$

The convergence of the algorithm is assessed by decreasing the cost functional and the reduction of the tracking errors E_1^k and E_2^k, which measure how well the computed state approaches the desired targets. The target functions ϕ_d and ϕ_T are chosen according to the desired control objective. We will consider several examples of simulations as follows

7.1. Example 1

The numerical values used in the simulations are summarized in Table 2. These parameters are chosen to ensure the stability of the finite difference scheme and convergence of the iterative algorithm.

Before presenting the numerical results, we briefly discuss the stability of the explicit finite difference scheme. Since the state equation contains the fourth-order term $\Delta^2\phi$, the stability of the method is strongly affected by the ratio

$$r = \frac{\eta(\Delta t)^2}{(\Delta x)^4}.$$

For the numerical values given in Table 2, we have

$$\Delta x = \frac{1}{40} = 2.5 \times 10^{-2}, \qquad \Delta t = \frac{1}{20000} = 5 \times 10^{-5}.$$

Therefore,

$$r = \frac{10^{-6}(5 \times 10^{-5})^2}{(2.5 \times 10^{-2})^4} = 6.4 \times 10^{-9}.$$

This value is very small, which helps to avoid the numerical instability generated by the biharmonic operator. Moreover, the gradient descent step size is chosen as $\tau = 2 \times 10^{-7}$, which is also small enough to prevent large oscillations in the control update. The maximum number of iterations is fixed as $K_{\max} = 300$, while the stopping tolerance is $\varepsilon = 10^{-5}$. These choices provide a stable numerical setting for the simulations.

Figures 1 and 2 illustrate that the calculated state $\phi^k(x,t)$, obtained after $k = 150$ iterations, closely matches the desired state $\phi_d(x,t)$. This is confirmed by the decrease of the error $E_1^k = 2.871 \times 10^{-4}$ and the bounded behavior of the control energy $\|p^k\|^2 = 2.028 \times 10^{-7}$.

Figure 3 demonstrates an accurate reconstruction of the terminal target $\phi_T(x)$ by the computed state $\phi^k(x,T)$. The small value of the error $E_2^k = 2.019 \times 10^{-5}$ and the controlled magnitude of the energy $\|p^k\|^2 = 2.028 \times 10^{-7}$ highlight the efficiency and stability of the proposed method.

Table 2. Numerical parameters used in the first example of simulations.

Symbol	Value	Description
L	1	Length of the spatial domain
T	1	Final time
N_x	40	Number of spatial grid points
N_t	20000	Number of time steps
η	10^{-6}	Biharmonic diffusion coefficient
α_1	1	Distributed tracking weight
α_2	1000	Terminal tracking weight
λ	80	Source feedback parameter
τ	2×10^{-7}	Gradient descent step size
$K_{\max}$	300	Maximum number of iterations
ε	10^{-5}	Stopping tolerance
p^0	0	Initial control
$\phi_d(x,t)$	$e^{-t}x^2(1-x)^2$	Desired state
$\phi_T(x)$	$e^{-1}x^2(1-x)^2$	Terminal target

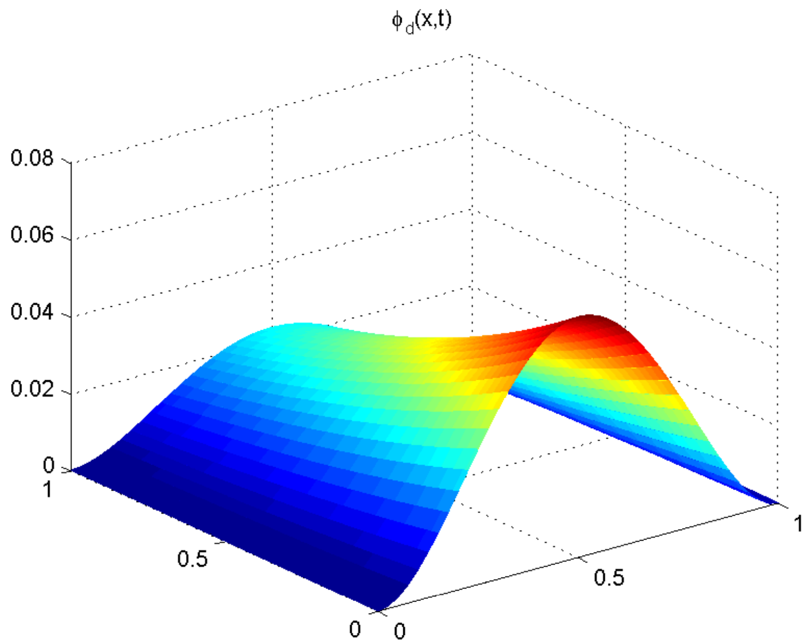

Figure 1. Desired state $\phi_d(x,t)$ representing a smooth decaying profile used as the control target.

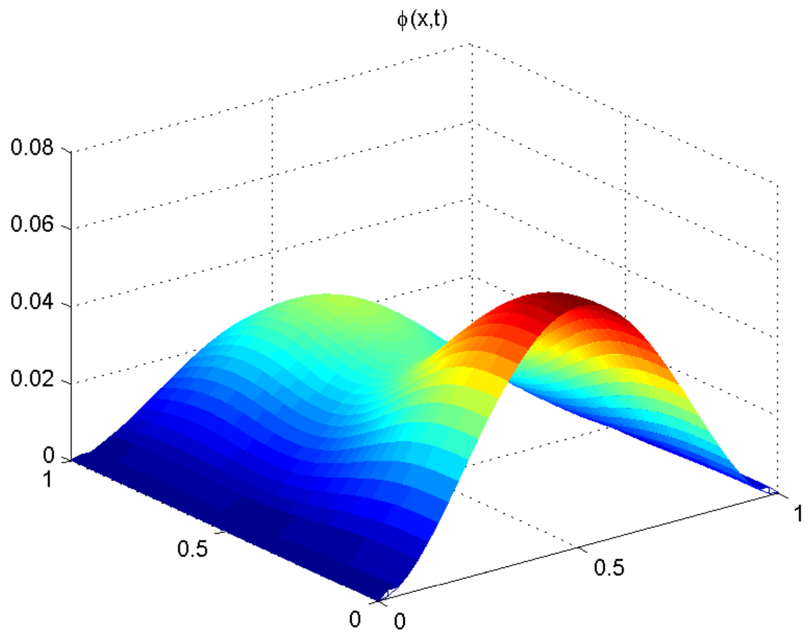

Figure 2. Computed state $\phi^k(x,t)$ at the convergence iteration $k = 150$.

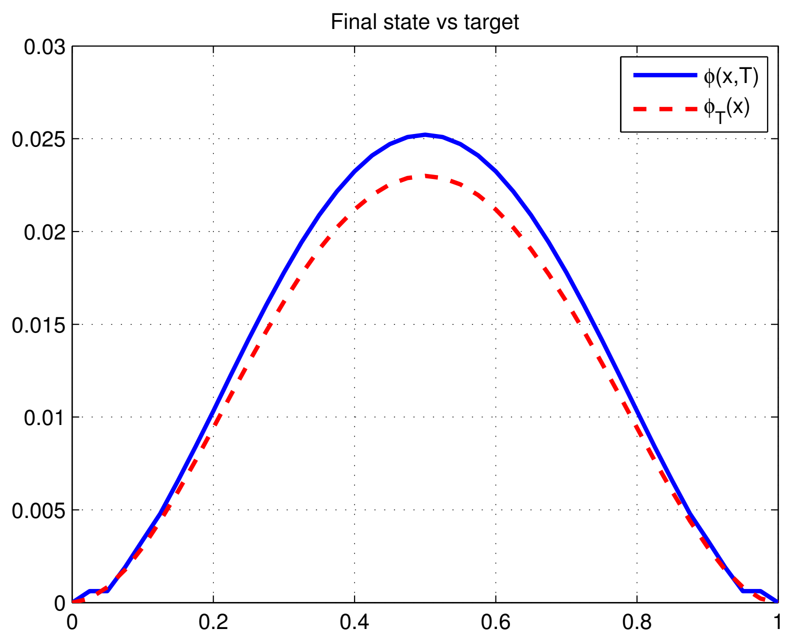

Figure 3. Final state $\phi^k(x,T)$ and terminal target $\phi_T(x)$ after $k = 150$ iterations, showing good agreement between the computed solution and the desired profile.

Table 3 reports the evolution of the tracking errors and the control energy during the last iterations.

We observe a clear decrease of both errors, especially E_1^k, which drops from 5.506×10^{-3} to 2.871×10^{-4}. Similarly, the terminal error E_2^k decreases to 2.019×10^{-5}, showing that the final state approaches the terminal target. The control energy $\|p^k\|^2$ also remains small, indicating that the desired precision is achieved with a moderate control effort.

Table 3. Convergence history of the algorithm over the last iterations of the first example.

Iter	E_1^k	E_2^k	$\|p^k\|^2$
145	5.506×10^{-3}	4.322×10^{-4}	1.894×10^{-5}
146	5.332×10^{-3}	4.221×10^{-4}	1.921×10^{-5}
147	4.223×10^{-3}	3.043×10^{-4}	1.947×10^{-6}
148	3.554×10^{-3}	3.251×10^{-5}	1.974×10^{-6}
149	3.234×10^{-3}	2.035×10^{-5}	2.001×10^{-6}
150	2.871×10^{-4}	2.019×10^{-5}	2.028×10^{-7}

7.2. Example 2

The numerical configuration adopted in the first simulation is reported in Table 4. In this example, the spatial domain is the interval $(0, 1)$ and the final time is fixed at $T = 1$. The discretization is performed with $N_x = 40$ spatial subintervals and $N_t = 20000$ time steps. Hence,

$$\Delta x = \frac{1}{40} = 2.5 \times 10^{-2}, \qquad \Delta t = \frac{1}{20000} = 5 \times 10^{-5}.$$

The state equation involves a fourth-order diffusion term. Therefore, the explicit finite difference approximation is sensitive to the quantity

$$r = \frac{\eta(\Delta t)^2}{(\Delta x)^4}.$$

Using the values $\eta = 10^{-6}$, $\Delta x = 2.5 \times 10^{-2}$, and $\Delta t = 5 \times 10^{-5}$, we obtain

$$r = \frac{10^{-6}(5 \times 10^{-5})^2}{(2.5 \times 10^{-2})^4} = 6.4 \times 10^{-9}.$$

Equivalently, the biharmonic stability indicator used in the implementation is

$$16r = 1.024 \times 10^{-7}.$$

This value is very small, which indicates that the time step is sufficiently small with respect to the fourth-order spatial discretization.
The linear source coefficient is chosen as

$$\lambda = -1.4.$$

Thus, the source contribution contains a damping part $\lambda\phi$, which helps to control the growth of the numerical solution. The corresponding contribution in the stability indicator is

$$|\lambda|(\Delta t)^2 = 1.4(5 \times 10^{-5})^2 = 3.5 \times 10^{-9}.$$

Consequently,

$$16\frac{\eta(\Delta t)^2}{(\Delta x)^4} + |\lambda|(\Delta t)^2 = 1.059 \times 10^{-7},$$

which remains far below the usual critical bound for the explicit scheme.
Since the control appears both in the bilinear transport term $-p\phi_x$ and in the additive term $+p$, we also restrict the admissible magnitude of the control by taking $p_{\max} = 30$. The associated transport indicator is

$$\frac{p_{\max}\Delta t}{\Delta x} = \frac{30(5 \times 10^{-5})}{2.5 \times 10^{-2}} = 6 \times 10^{-2}.$$

This value is smaller than one, which prevents the advective part from producing a numerical instability. These choices provide a stable computational setting for the finite difference scheme and allow the descent algorithm to update the control while avoiding excessive oscillations.

Table 4. Numerical parameters used in the second example of simulations.

Symbol	Value	Description
L	1	Length of the spatial domain
T	1	Final time
N_x	40	Number of spatial grid points
N_t	20000	Number of time steps
η	10^{-6}	Biharmonic diffusion coefficient
α_1	1	Distributed tracking weight
α_2	2000	Terminal tracking weight
λ	-1.4	Linear source coefficient in $h = \lambda\phi + p$
β_p	10^{-4}	Control penalization parameter
τ_0	10^{-5}	Initial gradient descent step size
$\tau_{\min}$	10^{-14}	Minimum admissible step size
θ	0.5	Step-size reduction factor
$K_{\max}$	400	Maximum number of iterations
ε	10^{-6}	Stopping tolerance
$p_{\max}$	30	Bound imposed on the control
p^0	0	Initial control
$\phi_d(x,t)$	$e^{-t}\sin^2(\pi x)$	Desired state
$\phi_T(x)$	$e^{-1}\sin^2(\pi x)$	Terminal target

Figures 4 and 5 illustrate that the calculated state $\phi^k(x,t)$, obtained after $k = 200$ iterations, closely matches the desired state $\phi_d(x,t)$. This is confirmed by the decrease of the error $E_1^k = 1.022 \times 10^{-5}$ and the bounded behavior of the control energy $\|p^k\|^2 = 1.063 \times 10^{-6}$.

Figure 6 demonstrates an accurate reconstruction of the terminal target $\phi_T(x)$ by the computed state $\phi^k(x,T)$. The small value of the error $E_2^k = 3.144 \times 10^{-5}$ and the controlled magnitude of the energy $\|p^k\|^2 = 1.063 \times 10^{-6}$ highlight the efficiency and stability of the proposed method.

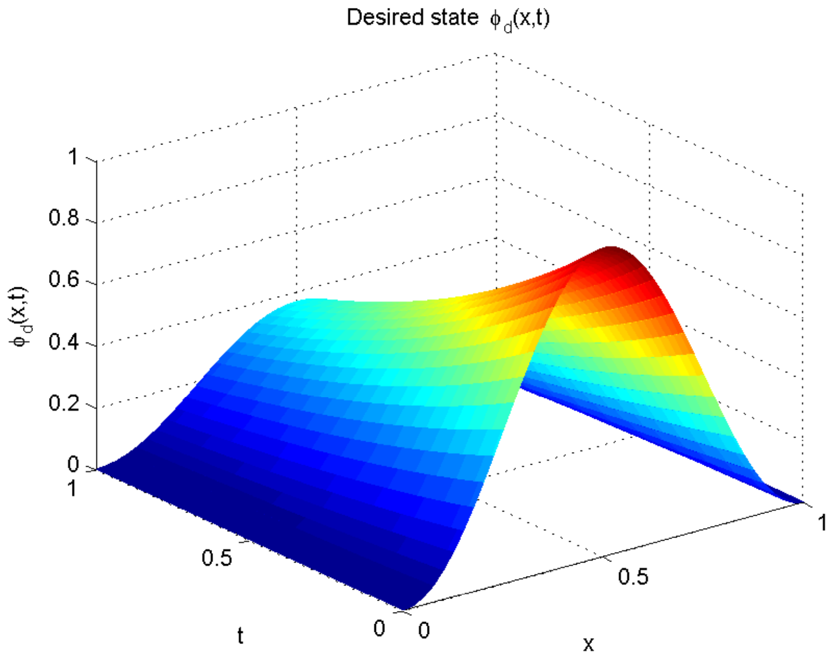

Figure 4. Desired state $\phi_d(x, t)$ representing a smooth decaying profile used as the control target.

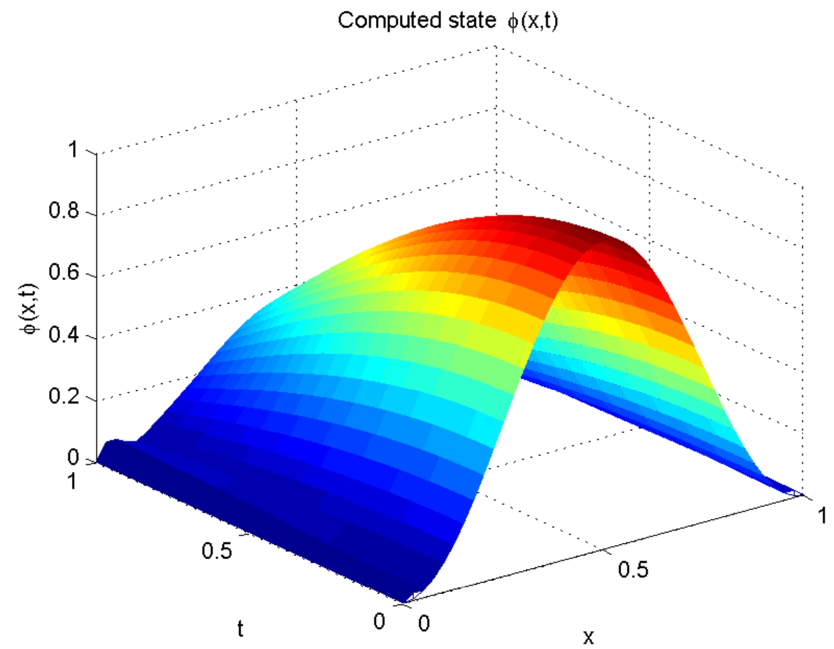

Figure 5. Computed state $\phi^k(x, t)$ at the convergence iteration $k = 200$.

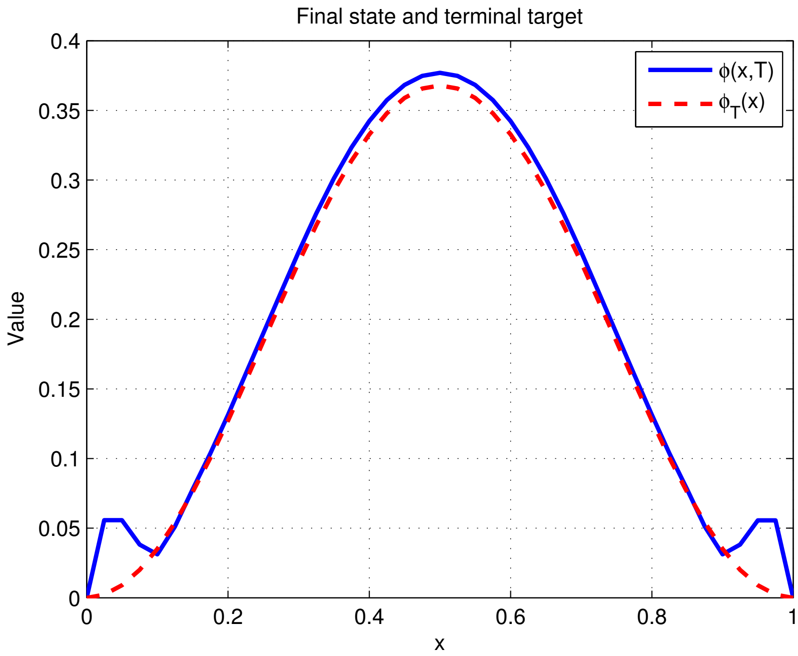

Figure 6. Final state $\phi^k(x,T)$ and terminal target $\phi_T(x)$ after $k = 200$ iterations, showing good agreement between the computed solution and the desired profile.

Table 5 reports the evolution of the tracking errors and the control energy during the last iterations of the second example. We observe a clear decrease of both errors, especially E_1^k, which drops from 1.045×10^{-4} to 1.022×10^{-5}. Similarly, the terminal error E_2^k decreases to 3.144×10^{-5}, showing that the final state approaches the terminal target. The control energy $\|p^k\|^2$ also remains small, indicating that the desired precision is achieved with a moderate control effort.

Table 5. Convergence history for the second numerical example.

Iteration	E_1^k	E_2^k	$\|p^k\|^2$
195	1.045×10^{-4}	5.341×10^{-4}	8.393×10^{-4}
196	1.038×10^{-4}	5.267×10^{-4}	9.480×10^{-4}
197	1.036×10^{-4}	4.431×10^{-5}	8.392×10^{-5}
198	1.031×10^{-4}	4.921×10^{-5}	9.479×10^{-5}
199	1.025×10^{-5}	3.151×10^{-5}	8.390×10^{-6}
200	1.022×10^{-5}	3.144×10^{-5}	1.063×10^{-6}

8. Discussion

The numerical experiments confirm the effectiveness of the proposed optimal control strategy for the fourth-order dynamical system under consideration. The two examples show that the controlled state approaches the desired profile with good accuracy, both in the distributed sense and at the terminal time. The convergence histories also show that the reduction of the tracking errors is obtained while the control energy remains small.

We first discuss the first numerical example. The convergence history reported in Table 3 shows a significant decrease of both the distributed error E_1^k and the terminal error E_2^k during the last iterations. More precisely, the distributed error decreases from 5.506×10^{-3} at iteration 145 to 2.871×10^{-4} at iteration 150. Similarly, the terminal error decreases from 4.322×10^{-4} to 2.019×10^{-5}.

This confirms that the algorithm improves the approximation of the desired trajectory and achieves a very accurate terminal matching. Moreover, the control energy remains small and decreases to the order of 10^{-7} at the last reported iteration. This indicates that the improvement of the tracking performance is not obtained through an excessive control effort.

The behavior observed in the first example is consistent with the structure of the controlled equation. The control acts through the transport-type term $p\phi_x$ and through the source contribution $+p$. Thus, it modifies both the propagation of the state and its amplitude. This explains the rapid reduction of the tracking errors in the final iterations. The small value of the control energy also shows that the penalization term plays its role in preventing large control values while still allowing the algorithm to improve the state approximation.

Next, we consider the second numerical example. The convergence history in Table 5 again confirms the efficiency of the proposed algorithm. In this case, the distributed error decreases to the order of 10^{-5}, while the terminal tracking error reaches the order of 10^{-5}. More precisely, at iteration 200, one obtains

$$E_1^{200} = 1.022 \times 10^{-5}, \qquad E_2^{200} = 3.144 \times 10^{-5}.$$

These values show that the final controlled state is very close to the terminal target. At the same time, the control energy remains of order 10^{-6} at the last iteration, which confirms that the convergence is achieved with a moderate control cost.

The comparison between the two examples shows that the proposed method gives stable and effective convergence in different numerical settings. In the first example, the reduction of the errors is particularly strong during the last iterations, with the terminal error reaching the order of 10^{-5}. In the second example, the convergence is even more accurate at the terminal time, since E_2^k reaches the order of 10^{-5}. These results support the robustness of the numerical strategy and show that the method is able to handle different target profiles while preserving a small control energy.

The choice of the numerical parameters plays an essential role in this behavior. In the second example, the spatial and temporal discretization parameters are fixed as $N_x = 40$ and $N_t = 20000$, which give

$$\Delta x = \frac{1}{40} = 2.5 \times 10^{-2}, \qquad \Delta t = \frac{1}{20000} = 5 \times 10^{-5}.$$

These values provide a fine temporal discretization, which is important for fourth-order evolution equations. Indeed, the presence of the biharmonic operator imposes a stronger stability restriction than in classical second-order diffusion problems. With $\eta = 10^{-6}$, the corresponding stability ratio is

$$r = \frac{\eta(\Delta t)^2}{(\Delta x)^4} = \frac{10^{-6}(5 \times 10^{-5})^2}{(2.5 \times 10^{-2})^4} = 6.4 \times 10^{-9}.$$

Equivalently, the biharmonic stability indicator used in the numerical implementation is

$$16r = 1.024 \times 10^{-7}.$$

This very small value indicates that the selected time step is sufficiently small with respect to the fourth-order spatial discretization. Consequently, the contribution of the biharmonic term does not generate numerical oscillations or instability.

The source coefficient is chosen as $\lambda = -1.4$ in the term $h = \lambda\phi + p$. Since λ is negative, this part of the source has a damping effect on the state. This choice is coherent with decreasing target profiles such as

$$\phi_d(x,t) = e^{-t}\sin^2(\pi x),$$

used in the second example. Hence, the damping produced by $\lambda < 0$ helps to prevent artificial growth of the numerical solution and contributes to the stability of the state equation. The contribution of this term to the stability indicator is

$$|\lambda|(\Delta t)^2 = 1.4(5 \times 10^{-5})^2 = 3.5 \times 10^{-9}.$$

Thus,

$$16\frac{\eta(\Delta t)^2}{(\Delta x)^4} + |\lambda|(\Delta t)^2 = 1.059 \times 10^{-7},$$

which remains very small.

The weights α_1 and α_2 determine the balance between the distributed and terminal tracking objectives. The distributed term controls the behavior of the state over the whole time interval, while the terminal term gives priority to the final-time approximation. In the second example, the choice $\alpha_1 = 1$ and $\alpha_2 = 2000$ gives strong importance to the terminal target, which explains the significant reduction of E_2^k observed in Table 5. This choice is also consistent with the goal of obtaining a precise final state while keeping the global tracking error controlled.

The parameter $\beta_p = 10^{-4}$ controls the penalization of the control energy. This small value allows the algorithm to use the control effectively, while still preventing the appearance of unnecessarily large controls. This is important because the control appears in the transport term $-p\phi_x$ and in the source contribution $+p$. If the control becomes too large, the transport term may introduce numerical oscillations. For this reason, the bound

$$p_{\max} = 30$$

is imposed on the control. The associated transport stability indicator is

$$\frac{p_{\max}\Delta t}{\Delta x} = \frac{30(5 \times 10^{-5})}{2.5 \times 10^{-2}} = 6 \times 10^{-2} < 1.$$

This confirms that the chosen bound is compatible with the stability of the explicit discretization.

The convergence of the optimization procedure is also influenced by the descent parameters. The initial step size is fixed as $\tau_0 = 10^{-5}$. This value is chosen to obtain effective progress in the cost functional without producing large oscillations in the control update. To improve robustness, an adaptive reduction strategy is used: whenever a trial update does not reduce the cost functional, the step size is multiplied by $\theta = 0.5$. The minimum admissible step is fixed as $\tau_{\min} = 10^{-14}$, which prevents the algorithm from continuing with numerically insignificant corrections. The stopping tolerance is $\varepsilon = 10^{-6}$, and the maximum number of iterations is $K_{\max} = 400$. These choices provide enough iterations for reducing the tracking errors while avoiding unnecessary computations once the improvement becomes negligible.

From the perspective of the working hypotheses, the results are consistent with the proposed control mechanism. The term $-p\phi_x$ allows the control to affect the spatial propagation of the state, whereas the contribution $+p$ improves the direct influence of the control on the amplitude. This combined action explains the decrease of both E_1^k and E_2^k in the two examples. The numerical results also show that this improvement is achieved with small values of $\|p^k\|^2$, which confirms the efficiency of the control strategy.

Compared with earlier works focused mainly on second-order diffusion equations, the present study addresses a fourth-order system, which is numerically and analytically more delicate. Fourth-order operators require stronger stability restrictions and a more careful discretization. Moreover, the present work is not limited to the standard first-order optimality framework. It also includes the characterization of the optimal control and the discussion of second-order optimality conditions. These elements strengthen the theoretical and numerical contribution of the study.

Overall, the numerical evidence supports the effectiveness of the proposed control framework for fourth-order dynamical systems. The selected parameters provide a good compromise between stability of the finite difference scheme, convergence of the descent algorithm, and efficiency of the control action. Future research may extend the method to two-dimensional domains, analyze the influence of the geometry and the control region, and compare the present descent strategy with more advanced optimization methods such as gradient descent or quasi-Newton algorithms.

9. Conclusions

In this work, we studied an optimal control problem for a second-order-in-time fourth-order dynamical system with advection effects. The control acts through the bilinear transport term $p \cdot \nabla\phi$, which allows it to influence the spatial evolution of the state. This setting is closely related to mathematical control theory for distributed parameter systems and provides a useful framework for the analysis of higher-order dynamical models. The proposed bilinear advection-control framework may be useful in real-world problems involving transport and diffusion phenomena, such as fluid flow control, pollutant dispersion, heat and mass transfer, and biological or environmental systems where the objective is to steer the state toward a desired profile with minimal control energy.

The first part of the paper was devoted to the mathematical analysis of the controlled state system. Under suitable assumptions on the data and the admissible controls, we established the well-posedness of the state equation. This result is essential because the optimal control problem is meaningful only when each admissible control generates a well-defined state.

We then formulated the associated optimal control problem and proved the existence of an optimal control by using the direct method of the calculus of variations. The optimality system was characterized through the derivation of the adjoint equation and the first-order necessary optimality condition. In addition, second-order necessary and sufficient optimality conditions were discussed in order to provide a refined characterization of local optimal solutions.

The numerical part illustrated the performance of the proposed approach. A finite difference scheme was used to approximate the state and adjoint equations, and a gradient-based iterative method was implemented to compute the control. The numerical examples showed a reduction of both the distributed tracking error and the terminal tracking error, while the control energy remained small. These results indicate that the proposed strategy can drive the state toward prescribed targets with moderate control effort.

The simulations also confirmed the importance of the numerical parameters in the stability and convergence of the algorithm. In particular, the time step, the biharmonic diffusion coefficient, the tracking weights, and the descent step size play important roles in the behavior of the scheme. Since the biharmonic operator imposes stronger stability restrictions than standard second-order diffusion operators, a careful choice of discretization parameters is required.

Compared with optimal control problems governed by second-order diffusion equations, the present study deals with a more delicate higher-order dynamical system. The fourth-order operator and the bilinear advection term introduce additional analytical and numerical difficulties. Therefore, the obtained results contribute to the study of optimal control for higher-order distributed parameter systems and are aligned with recent developments in dynamical systems and mathematical control theory.

Future work may consider several extensions and address some limitations of the present study. First, the analysis developed here is restricted to a linear fourth-order system on a finite-time horizon. A natural extension is the study of semilinear fourth-order systems under suitable regularity and growth assumptions on the nonlinear term. Another important direction is the infinite-horizon case, which would require additional dissipativity, stabilization, or discounting assumptions. Second, the proposed numerical approach may be extended to two-dimensional and multidimensional domains, where the treatment of the divergence-free constraint and the construction of efficient algorithms become more delicate. Third, the influence of the geometry of the domain and the location of the control region may be analyzed. Fourth, faster optimization methods, such as gradient descent or quasi-Newton algorithms, may be used to improve computational efficiency. Finally, other control mechanisms may be compared with the present bilinear advection control in order to clarify their influence on the performance of the controlled system.

Author contributions

All authors contributed equally to this work.

Use of Generative-AI tools declaration

The authors declare they have not used Artificial Intelligence (AI) tools in the creation of this article.

Data availability

The simulated data used in the article are available from the corresponding author.

Acknowledgments

Nouf A. Alrubea & Maawiya Ould Sidi would like to thank Jouf University for their support.

Conflicts of interest

The authors declare that they have no conflict of interest.

References

1. I. Lasiecka, Stabilization of hyperbolic and parabolic systems with nonlinearly perturbed boundary conditions, *J. Differ. Equations*, **75** (1988), 53–87. https://doi.org/10.1016/0022-0396(88)90129-5
2. J. Lagnese, J. L. Lions, *Modelling analysis and control of thin plates*, Recherches En Mathématiques Appliquées, 1988.
3. J. E. Lagnese, *Boundary stabilization of thin plates*, SIAM, 1989. https://doi.org/10.1137/1.9781611970821
4. J. E. Lagnese, G. Leugering, E. J. P. G. Schmidt, *Modeling, analysis and control of dynamic elastic multi-link structures*, Systems & Control: Foundations & Applications; Birkhäuser: Boston, MA, USA, 1994. https://doi.org/10.1007/978-1-4612-0273-8
5. X. Li, J. Yong, *Optimal control theory for infinite dimensional systems*, Systems & Control: Foundations & Applications; Birkhäuser: Boston, MA, USA, 1995.
6. F. Tröltzsch, *Optimal control of partial differential equations: Theory, methods and applications*, Graduate Studies in Mathematics, Vol. 112; American Mathematical Society: Providence, RI, USA, 2010.
7. J. L. Lions, E. Magenes, *Non-homogeneous boundary value problems and applications*, Vol. 1, Springer: Berlin/Heidelberg, Germany, 1972.
8. R. A. Adams, *Sobolev spaces*, Academic Press, 1975.
9. M. Bradley, S. Lenhart, Bilinear optimal control of a Kirchhoff plate, *Syst. Control Lett.*, **22** (1994), 27–38. https://doi.org/10.1016/0167-6911(94)90023-X
10. M. Bradley, S. Lenhart, J. Yong, Bilinear optimal control of the velocity term in a Kirchhoff plate equation, *J. Math. Anal. Appl.*, **238** (1999), 451–467. https://doi.org/10.1006/jmaa.1999.6524
11. R. Prakash, Optimal control problem for the time-dependent Kirchhoff-Love plate in a domain with rough boundary, *Asymptotic Anal.*, **81** (2013), 337–355. https://doi.org/10.3233/ASY-2012-1132
12. I. Bock, I. Hlaváček, J. Lovíšek, On the optimal control problem governed by the equations of von Kármán. II. Mixed boundary conditions, *Apl. Mater.*, **30** (1985), 375–392. https://doi.org/10.21136/AM.1985.104164
13. J. Y. Park, S. H. Park, Y. H. Kang, Bilinear optimal control of the velocity term in a von Kármán plate equation, *ANZIAM J.* **54** (2013), 291–305. https://doi.org/10.1017/S1446181113000205
14. J. Hwang, Optimal control problems for a von Kármán system with long memory, *Bound. Value Probl.*, **2016** (2016), 87. https://doi.org/10.1186/s13661-016-0594-7
15. M. Bradley, Uniform stabilization of a nonlinearly perturbed Kirchhoff plate, *Appl. Math. Optim.*, **26** (1992), 1–19.
16. A. Favini, M. A. Horn, I. Lasiecka, D. Tataru, Global existence, uniqueness and regularity of solutions to a von Karman system with nonlinear boundary dissipation, *Differ. Integral Equ.*, **9** (1996), 267–294. https://doi.org/10.57262/die/1367603346
17. A. Preumont, *Vibration control of active structures: An introduction*, 3 Eds., Solid Mechanics and Its Applications, Vol. 179, Springer: Dordrecht, The Netherlands, 2011.

18. Y. Liu, H. Matsuhisa, H. Utsuno, Semi-active vibration isolation system with variable stiffness and damping control, *J. Sound Vib.*, **313** (2008), 16–28. https://doi.org/10.1016/j.jsv.2007.11.045

19. M. Alhazmi, M. O. Sidi, Bilinear optimal control problem with minimum energy for a fourth-order reaction diffusion system, *AIMS Math.*, **11** (2026), 10274–10310. https://doi.org/10.3934/math.2026425

20. E. Zerrik, A. El Kabouss, Regional optimal control of a bilinear wave equation, *Int. J. Control*, **92** (2019), 940–949. https://doi.org/10.1080/00207179.2017.1375158

21. E. H. Zerrik, A. A. Aadi, M. Ouhafsa, On the regional tracking problem of the bilinear wave equation subject to bounded controls, *Eur. J. Control*, **76** (2024), 100943. https://doi.org/10.1016/j.ejcon.2023.100943

22. A. A. Aadi, E. H. Zerrik, Constrained regional control problem of a bilinear plate equation, *Int. J. Control*, **95** (2022), 996–1002. https://doi.org/10.1080/00207179.2020.1834144

23. S. Lenhart, D. Wilson, Optimal control of a heat transfer problem with convective boundary condition, *J. Optim. Theory Appl.*, **79** (1993), 581–597. https://doi.org/10.1007/BF00940560

24. E. H. Zerrik, A. El Kabouss, *Bilinear boundary control problem of an output of parabolic systems*, In: Recent Advances in Modeling, Analysis and Systems Control: Theoretical Aspects and Applications, Springer: Cham, Switzerland, 2020, 193–203. https://doi.org/10.1007/978-3-030-26149-8_15

25. E. Zerrik, A. El Kabouss, *Regional optimal control problem of a heat equation with bilinear bounded boundary controls*, In: Recent advances in intuitionistic fuzzy logic systems and mathematics, Springer, 2021, 131–142. https://doi.org/10.1007/978-3-030-53929-0_10

26. M. Liang, Bilinear optimal control for a wave equation, *Math. Mod. Meth. Appl. S.*, **9** (1999), 45–68.

27. A. Kröner, K. Kunisch, B. Vexler, Semismooth Newton methods for optimal control of the wave equation with control constraints, *SIAM J. Control Optim.*, **49** (2011), 830–858. https://doi.org/10.1137/090766541

28. K. Kunisch, P. Trautmann, B. Vexler, Optimal control of the undamped linear wave equation with measure valued controls, *SIAM J. Control Optim.*, **54** (2016), 1212–1244. https://doi.org/10.1137/141001366

29. M. Gugat, V. Grimm, Optimal boundary control of the wave equation with pointwise control constraints, *Comput. Optim. Appl.*, **49** (2011), 123–147.

30. J. Liu, J. W. Pearson, Parameter-robust preconditioning for the optimal control of the wave equation, *Numer. Algorithms*, **83** (2020), 1171–1203. https://doi.org/10.1007/s11075-019-00720-y

31. C. Clason, K. Kunisch, P. Trautmann, Optimal control of the principal coefficient in a scalar wave equation, *Appl. Math. Optim.*, **84** (2021), 2889–2921. https://doi.org/10.1007/s00245-020-09733-9

32. E. Casas, F. Tröltzsch, Second order analysis for optimal control problems: Improving results expected from abstract theory, *SIAM J. Optim.*, **22** (2012), 261–279. https://doi.org/10.1137/110840406

33. M. S. Aronna, F. Tröltzsch, First- and second-order optimality conditions for the control of Fokker–Planck equations, *ESAIM Control Optim. Calc. Var.*, **27** (2021), 15. https://doi.org/10.1051/cocv/2021014
34. R. El Mezegueldy, S. Yahyaoui, M. Ouzahra, Infinite-horizon optimal control of a locally controlled Fokker–Planck equation, *SeMA J.*, **83** (2025), 293–316. https://doi.org/10.1007/s40324-025-00393-9
35. N. Beheshti, M. Rezanejad, M. Mehrasa, Linearized control technique with Lyapunov function-based compensators for MMC-based HVDC system under load variation and fault condition, *Int. J. Elec. Power*, **124** (2021), 106333. https://doi.org/10.1016/j.ijepes.2020.106333
36. A. Cheddour, A. Elazzouzi, A new decomposition method approach for strong and exponential stabilization of semilinear systems in Banach spaces, *NODEA-Nonlinear Differ.*, **33** (2026). https://doi.org/10.1007/s00030-025-01173-0
37. J. Masoliver, Telegraphic transport processes and their fractional generalization: A review and some extensions, *Entropy*, **23** (2021), 364. https://doi.org/10.3390/e23030364
38. S. Akbari, S. Faghiri, P. Poureslami, K. Hosseinzadeh, M. B. Shafii, Analytical solution of non-Fourier heat conduction in a 3-D hollow sphere under time-space varying boundary conditions, *Heliyon*, **8** (2022), e12496. https://doi.org/10.1016/j.heliyon.2022.e12496
39. R. J. LeVeque, *Finite difference methods for ordinary and partial differential equations: Steady-state and time-dependent problems*, SIAM: Philadelphia, PA, USA, 2007.

AIMS Press